JPRS-CST-84-024

23 August 1984

China Report

SCIENCE AND TECHNOLOGY

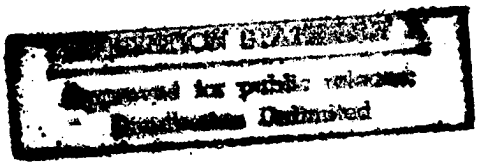

FBIS FOREIGN BROADCAST INFORMATION SERVICE

NOTE

JPRS publications contain information primarily from foreign newspapers, periodicals and books, but also from news agency transmissions and broadcasts. Materials from foreign-language sources are translated; those from English-language sources are transcribed or reprinted, with the original phrasing and other characteristics retained.

Headlines, editorial reports, and material enclosed in brackets [] are supplied by JPRS. Processing indicators such as [Text] or [Excerpt] in the first line of each item, or following the last line of a brief, indicate how the original information was processed. Where no processing indicator is given, the information was summarized or extracted.

Unfamiliar names rendered phonetically or transliterated are enclosed in parentheses. Words or names preceded by a question mark and enclosed in parentheses were not clear in the original but have been supplied as appropriate in context. Other unattributed parenthetical notes within the body of an item originate with the source. Times within items are as given by source.

The contents of this publication in no way represent the policies, views or attitudes of the U.S. Government.

PROCUREMENT OF PUBLICATIONS

JPRS publications may be ordered from the National Technical Information Service, Springfield, Virginia 22161. In ordering, it is recommended that the JPRS number, title, date and author, if applicable, of publication be cited.

Current JPRS publications are announced in Government Reports Announcements issued semi-monthly by the National Technical Information Service, and are listed in the Monthly Catalog of U.S. Government Publications issued by the Superintendent of Documents, U.S. Government Printing Office, Washington, D.C. 20402.

Correspondence pertaining to matters other than procurement may be addressed to Joint Publications Research Service, 1000 North Glebe Road, Arlington, Virginia 22201.

JPRS-CST-84-024

23 August 1984

CHINA REPORT

SCIENCE AND TECHNOLOGY

CONTENTS

PEOPLE'S REPUBLIC OF CHINA

ABSTRACTS

APPLIED SCIENCES

'Y-12' DEMONSTRATION FLIGHT DETAILED

Beijing HANGKONG ZHISHI [AEROSPACE KNOWLEDGE MAGAZINE] in Chinese No 6, Jun 84 pp 6-7

[Article by Song Chaolin [1345 2600 2651]]

[Text] It was an unusually clear day on the morning of 16 March. We drove to the airport to see the demonstration flight of China's newest multi-purpose light aircraft, the Y-12.

Observing the Flight Demonstration

As we stepped out of the car, it was apparent that preparation work for the flight demonstration had been completed. A member of the working crew pointed out the Y-12 to me. It was decorated in red and blue ribbons.

In a short while, the engines were started, and the Y-12 began rolling toward the runway. When it reached the runway, the aircraft's speed increased; after accelerating for about 100 meters the front wheel began lifting off the ground, and the aircraft headed straight toward the sky. After circling the airfield, the aircraft made a diving pass over the airport at a speed of 180 km/hr and an altitude of 10 meters, then it began climbing and circling at a rate of more than 6.5 m/sec, like a swallow dancing in the air. When the Y-12 again began its dive, six or seven photographers rushed toward the aircraft, hoping to capture a few action shots of the dive and the low-altitude run. This time, the altitude was even lower and the speed even higher.

Having completed this maneuver, the nose of the aircraft suddenly pulled up, and the ship went into a rapid climb, then again flew away from the airport. Several minutes later, it landed on the runway; traveling approximately 100 meters after touchdown, it came to a complete stop. "How come the landing distance is so short?" someone asked. To answer this question, Deputy Director Yang Shouwen of the Weijian Machinery Plant, builder of the Y-12, gave the following explanation: "This is the last event of today's flight demonstration--prop reversal on landing." Propeller reversal means that at the instant the aircraft touches the ground, the pilot quickly activates a control to change the angle of the propeller blade from positive to negative; the reverse thrust thus generated by the propellers greatly reduces the landing distance required. The largest negative angle of the Y-12 propeller blades is 15°, and the corresponding landing distance is only about 200 meters. This is the first time propeller reversal techniques have been used on a Chinese-built aircraft.

The flight demonstration was a success. The superior performance exhibited by the Y-12 received very good comments from the spectators.

As soon as the aircraft came to a stop on the field, it was surrounded by the crowd. Although the weather was bad, everyone's spirit was high. Some were lightly touching the aircraft body; others had cornered the flight crew to inquire about their experience; still others were trying to board the aircraft for a tour. The enthusiasm of the crowd fully illustrated the people's admiration for this Chinese-built aircraft.

A Conversation With Deputy Director Yang

We invited Deputy Director Yang Shouwen of the Weijian Machinery Plant, who was in charge of production, to discuss the structure and performance of the Y-12. This was his statement: The Y-12 has two engines, single high wing, single vertical tail, and fixed, tricyle type landing gear. The aircraft's rectangular wing is of a double spar structure with side support struts. The airfoil type is GA-0417 with a thickness ratio of 17 percent. At the trailing edge of the inner wing section is a Fowler flap; at the outer section is an aileron. Inside the wing is an integral fuel tank with a maximum capacity of 1,254 kg. The vertical tail is trapezoidal in shape and the horizontal tail is rectangular. The cockpit is large enough to accommodate two pilots; the pilots' seats can be adjusted forward and backward as well as vertically. The central control panel is located in front of and between the two seats. The cockpit has a cargo door on the left side, and also a door behind the pilots leading to the passenger (cargo) cabin. During flight, the left cargo door can be opened freely or even removed for parachuting or dropping supplies. The instrument panel includes navigation instruments as well as a complete set of engine monitoring gauges and other operating instruments. A variety of electronic equipment can also be installed which include ultra shortwave radio, intercom, shortwave radio, radio compass, radio altimeter, and beacon receiver. The aircraft is also equipped with night-flying instruments.

"What is the difference between Y-12 and Y-11?" someone else asked.

Yang gave the following reply. The Y-11 was a multi-purpose aircraft developed in 1975 primarily for agricultural and forestry applications.

In recent years, it had been used for spraying insecticides in many regions including Xinjiang, Nei Monggol, the three northeast provinces, Tangshan and Guangzhou. The treated area was as large as several million mu, and the results were very effective. Actual experience with the Y-11 during the last few years has proved that it is a very good aircraft. The Y-12 was developed based on the experience in building the Y-11 and based on considerations of demands in domestic and overseas markets. Compared to the Y-11, the Y-12 is longer and taller, and its wing has a new airfoil design. Its performance is also significantly improved. The Y-11 has two piston type engines, each rated at only 285 hp; the Y-12 is equipped with two Canadian-built PT6 propeller engines, each rated at 500 hp (model 1) or 620 hp (model 2). The Y-11 has a maximum payload of 800 kg and a passenger capacity of eight persons. The Y-12 has a maximum payload of 1,700 kg

and passenger capacity of 17 persons. The maximum range of the Y-11 is 1,140 km compared to 1,440 km for the Y-12. In addition, the Y-12 uses propeller reversal on landing and has the capability of single-engine take-off and single-engine climb.

Development of the Y-12

The design work of the Y-12 began in 1980; preliminary design was completed after the first quarter of that year. It was first test flown on 14 July 1982, and static tests were completed during the same year. The design, ground testing and flight tests of the Y-12 were carried out according to international flight regulations. Currently, the aircraft is in small-scale production.

During the development process, engineers and technicians overcame various difficulties and solved a number of challenging technical problems. Many new technologies such as integral ribs, wall panels, integral fuel tanks, and epoxy and rivet joints were successfully applies in the design. The Y-12 has now accumulated over 400 flight hours. This demonstration aircraft flew directly from Harbin to Beijing; the total flight time was 4.5 hours. The aircraft had good stability and control characteristics. Since arriving in Beijing, it has flown missions for geological exploration over the Chende region. Flying geological exploration missions requires that the aircraft maintain a relative altitude of less than 100 meters above the terrain. When the difference in elevation between peaks and valleys exceeds 400 meters, the aircraft must be able to climb and dive rapidly to maintain an altitude of 100 meters. After 5 hours of continuous operation, the geological department was completely satisfied with the Y-12's performance. Deputy Director Yang indicated that a series of ground and flight tests have shown that the performance of the Y-12 has reached the standard of foreign aircraft of the same class. After the demonstration in Beijing, the Y-12 will return to the factory and continue its flight test program so that it can be delivered to the users at the earliest possible date.

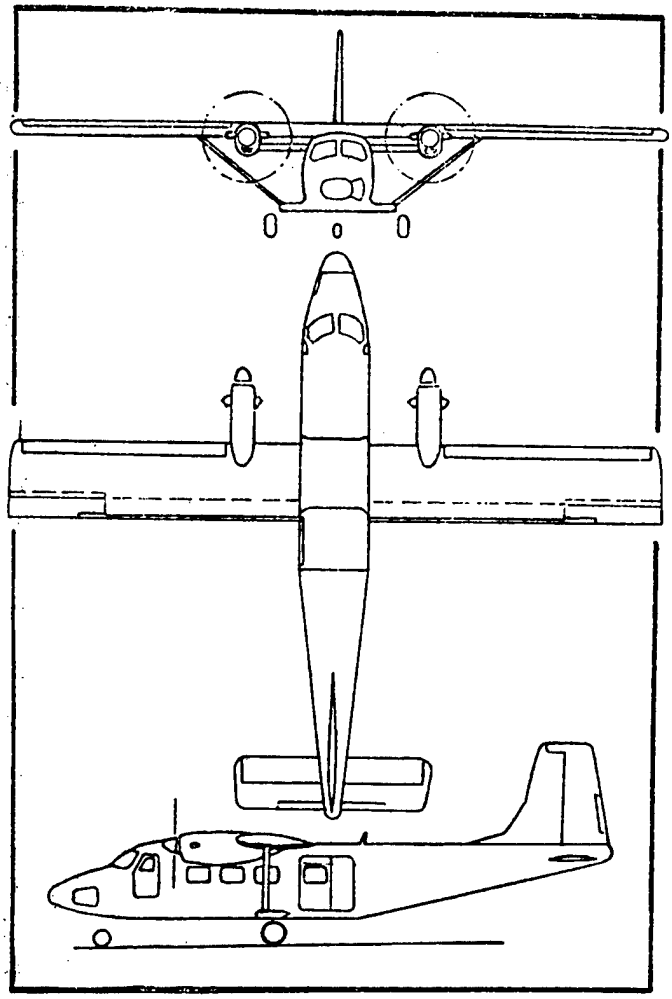

3012
CSO: 4008/350

OUTLINE OF DEVELOPMENT OF CHINA'S URANIUM MINING TECHNOLOGY AND SUGGESTIONS FOR ITS IMPROVEMENT

Beijing HE KEXUE YU GONGCHENG [CHINESE JOURNAL OF NUCLEAR SCIENCE AND ENGINEERING] in Chinese No 3, Sep 82 pp 255-261

[Article by Wang Jian [3769 7002], Li Yunfeng [2621 5686 1496], and Liu Enchong [0491 1869 0339] (Ministry of Nuclear Industry)]

[Abstract] This paper analyzes specific features of China's uranium mining technology and reviews the development of China's mining technology in general. Future technical development must be closely governed by economic considerations if past mistakes are to be avoided. Some suggestions for improving the technology are offered.

[Text]

1. INTRODUCTION

In the 23 years since China's first uranium mine was opened in 1958, China's uranium industry has constructed a full complement of uranium mines, hydrometallurgical plants, and appropriate research and planning institutes. A rather large body of technical experience has accumulated which can be adapted to all types of uranium ore mining. The capabilities of the nuclear raw materials industry have expanded enormously through reliance on China's own technical resources and through the use of equipment and machinery built in China. Nevertheless, in certain technical and economic respects our position is still not ideal, and the products of China's uranium hydrometallurgy are not competitive in foreign markets. In connection with current efforts to adjust the national economy, we will now discuss the current state of China's uranium mining technology and explore some suggestions for further improvements.

2. SPECIFIC ASPECTS OF CHINA'S URANIUM ORE EXTRACTION TECHNOLOGY

Although there are many close similarities between uranium and other industrial mining techniques, uranium mining has some unique features. For example: 1) Uranium deposits are identified primarily through their radioactivity. 2) Protection from radiation is essential in uranium mines. 3) Uranium deposits are generally small and produce low-grade ore; hence, the costs of the products

of uranium hydrometallurgy are rather high. Thus, in addition to the special requirements with regard to geological prospecting, protective ventilation techniques, etc., special techniques are also required to extract uranium deposits. Uranium extraction technology in China can be characterized in more detail as follows:

1. The ore deposits are complex and of many types and may form in association with deposits of granite, volcanic rock, basin sediments, woolastonite [calcium silicate] mudstone, etc. As to the lithological character of the ore deposits, there may be quartzite, granite, lamprophyre, rhyolite, schist, slate, limestone, conglomerate rock, sandstone, coal deposits, etc. The ore deposits may be structurally very stable or extremely unstable, and the conditions of ore production vary widely. All this gives rise to factors which adversely affect mining and hydrometallurgical technologies.

2. The scale of ore deposits is small. About 70 percent of the ore being exploited by currently producing mines or mines under construction comes from small deposits. Most of the mines are small--only a few are of medium size.

3. Most of the ore bodies are thin and small, and they are irregularly distributed. Except for a few massive deposits, the ore bodies in most mines are both thin and widely scattered. The deposits may have lenticular form, or they may be stratified or contained in a thin vein or network of veins. Mining conditions are thus unfavorable since large-scale mining equipment cannot be used, mining efficiency is low, and the deposits are quickly exhausted. Most of the ore deposits are mineralized in a dispersed way. Defined reserves are distributed over rather large distances (particularly with regard to depth), so that the amount of ore present at each stage of exploitation is quite small. Each year during the extractive phase, tunneling footage must be increased, expanding the ratio of tunneling to mining. The total tunneling ratio in uranium mines is generally 40-60 meters per 1,000 tons (occasionally even exceeding 100 meters per 1,000 tons). This is 2-3 times as much as in the ordinary mine.

4. The shape of the ore body is complex and the profile of the deposits is difficult to determine accurately. The shapes of most uranium ore bodies are complex, with frequent bifurcations, complications, expansions and contractions. Rather dense exploratory networking and geological work are therefore required to explore the deposits fully. In some cases one has no choice but to mine and prospect at the same time because it may be difficult to obtain complete and precise information on the contours of the ore body even after extensive preliminary scouting. It is often necessary to change plans while mining is actually under way.

3. MINING TECHNIQUES

Owing to geological constraints, underground mining techniques predominate, accounting for 80-82 percent of total production. Open-pit mining accounts for the rest, and there can be no major changes here in the near future. Conventional strip-mining techniques are generally employed in open-pit mining.

Fill techniques account for 54-58 percent of underground mining (here and below, all estimates are based on yield). Caving methods are next in importance, accounting for 20-30 percent of production. Open-stope mining (including shrinkage stoping) accounts for 12-20 percent. These methods are summarized in detail in Table 1, and in the following sections we give a general description of the various mining techniques (cf. Table 2).

Table 1. Change in the Relative Yields (in percent) of Various Mining Techniques

		1966	1976	1978	1979	1980
Fill methods	Horizontal cut-and-fill	58	58.5	54.1	57.3	50.9
	Inclined cut-and-fill	--				3.3
Open-stope methods	Shrinkage stoping	12	10.2	8.2	9.2	7.1
	Completely open-stope method, and open-stope with shrinkage method	--	7.1	11.8	9.3	4.4
	Room-and-pillar method	--	--	--	--	2.8
Caving methods	Wall caving	29.3	16.4	15.4	15.6	17.7
	Slice caving	--	7.6	9.7	8.4	13.2
Square-set stoping		0.7	--	0.8	0.2	--
Other methods		--	0.2	--	--	0.6

1. Cut-and-fill technique for horizontal slices. This adaptible method is suited for various types of ore deposits and is characterized by relatively low ore dilution and loss. Because this safe method effectively controls ground-pressure movements and the safety and working conditions are favorable, it is widely employed in China's uranium mines. The method is well suited for simultaneous mining and exploration when the shape of the ore body is highly variable. Much experience has already been gained regarding stope layout and ore extraction techniques. The principal findings may be summarized as follows:

(1) Several fairly sophisticated design techniques have been worked out for the structure of the stope floor to ensure safety and raise the recovery rate during recovery of roof-to-floor pillars. For example, artificial concrete floors or tunnels can be constructed, or reinforced concrete pads can be added to natural floors and pillars.

(2) For the richer ore deposits, concrete walls are first poured to separate adjacent stopes; alternatively, pillars consisting of ore may be replaced by concrete pillars.

(3) After each slice has been completely mined and filled, ore dilution and pulverization losses can be avoided by laying down a concrete slab.

(4) A high-quality fill system, an adequate source of fill material, and sufficient storage space for fill material are all necessary, and there must also be a concrete preparation station and a pipeline system for transporting the concrete if prompt filling is to be ensured.

(5) Contamination of the downpit ventilation system by radon gas can be greatly decreased by filling the pits with poured concrete after mining rather than using prefabricated concrete pillars or other support structures.

(6) Ore yields can be effectively increased and mining costs reduced by centralized coordination of mining procedures. The average area of stope No 17 in the +180 central level of the Chenzhou Uranium Mine is equal to 350 m^2. A total of 17,000 tons of ore was extracted in a year from the top 13 slices of a stope 21 m high. The average monthly yield of ore, 4.8 t/m^2, was 20 percent higher than in ordinary mines, and direct mines costs were cut by 5.8 percent.

In most of the fill methods now in use, the stopes are dry-filled with waste rock obtained from the surface or with rubble generated by tunneling inside the pits. Roughly 25-33 percent of the total time required for mining is devoted to stope filling. In order to reduce this time, other filling methods are now being promoted in which a mixture of sand and water, cement, or other materials are used.

2. Cut-and-fill method for inclined slices. This technique is used to mine uranium where coal is present. The inclination angle exceeds 45° and the slice thickness ranges from 0.4 to 2 m. The stopes are laid out over a length of 15-50 m along the strike. After the ore is extracted, the excavated region is filled with waste tunneling rock or gobi gravel. An iron chute (or similar device) is employed on the fill-material slide to facilitate removal of ore from the mine. In the future, mining efficiency should be improved by making the stopes as long as possible and putting mining activities under more centralized control.

3. Wall caving. This is used mainly to mine thin, gently inclined seams of thickness 0.2-2.8 m and inclination 10°-17°. The workface length is 20-50 m, and supporting structures are constructed as needed during mining. As the workface advances, supporting pillars are removed at the rear so that the roof collapses under its own weight. Wooden pillars have been used, but plans are underway to introduce metal pillars. Techniques for rapidly mining narrow seams of ore are currently being tested for slices less than 1 m wide.

4. Slice caving. This method is used mainly to extract ore from structurally unstable mines. Metal pillars are being tested as replacements for wood pillars (sets) in order to reduce wood consumption. Studies are in progress to find ways of increasing the number of times the metal pillars can be reused so as to bring costs down. However, the low efficiency and the difficulty in providing adequate ventilation are serious unsolved drawbacks of this method.

Table 2. Outline of the Various Important Mining Techniques

	Cut-and fill methods		Open-stope methods		Caving Methods	
	Horizontal cut-and-fill	Inclined slice cut-and-fill	Shrinkage stopings and open-stope with shrinkage	Completely open-stope and room-and-pillar methods	Wall caving	Slice caving
Principal equipment used	Roof drills, electric hoes (in a few cases, rock-drilling platform-cars, pneumatic loader-conveyors, etc.)	Electric coal drills	Jackhammer drills, roof drills, electric hoes	Jackhammer drills, electric hoes	Jackhammer drills, electric hoes	Jackhammer drills, Hand-guided pneumatic hoes
Means of support	---	Wooden supports	---	Rock or ore pillars	Wooden supports	Wooden supports, metal nets, metal pillars
Monthly stope production capacity (tons)	630-1200	490-670	720-1000	250-800	940-1080	530-750
Output per mining shift (tons)	2.4-5.2	1.3-1.6	2-6.3	2.9-4.2	1.8-2	1.7-2
Ore loss rate (percent)	2-5	6-10	3-8	5-20	1.4-2	7-8
Ore dilution rate (percent)	10-18	24-30	30-36	20-25	30-36	10-16.5
Principal remaining problems	Much time and labor required to find side slopes and clear bottoms	Low production capacity and efficiency, high wood consumption	Demands high degree of ventilation	High loss rate	Inefficient, consumes much wood, high ore dilution	High wood consumption, low efficiency, ventilation difficult

5. Shrinkage stoping. This method is suitable only for regular veins which are steeply inclined and have stable tops. Ore processing is simple and the work capacity and efficiency are rather high. Obstruction of the vein by large rocks can be avoided by using an electric hoe equipped with a chute at the bottom. Since a large amount of ore is usually piled up inside the mining chamber, a rather large amount of radon gas may be released. Partial downward ventilation is effective in ensuring that safety conditions at the worksite are up to standard.

6. Completely open-stope method. This method requires a gently sloping ore body of at most moderate thickness. The roof must be structurally stable; if the deposit is of large area, suitably located pillars must be used to support the stope. This can be done either by using pillars consisting of low-grade ore or by pouring concrete to form artificial pillars.

4. OPENING UP AND DRIVING OF NEW MINES

In the mines currently in production, 27 percent were opened by vertical shafts, 68 percent by inclined shafts, and 5 percent by horizontal drifts. The vertical shafts are 127-313 meters deep with an average depth of 224 meters. The shafts are usually equipped with double-drum windlasses 2-2.5 meters in diameter and with cage hoists. A few vertical shafts are equipped with multi-rope windlasses with friction wheels of diameter 1.85 meters. The slant length of the inclined shafts averages 297 meters, and the mine car parks employ uncoupling cars and tracks in most of these shafts, although cable-suspension-type cars are also employed in a few cases. Along the horizontal drifts, electric trolley locomotives or storage battery locomotive are used for transportation.

Blower fans provide forced air for ventilation in 32 percent of the mine shafts; exhaust fans are used in the other 68 percent. In the former case, it is stipulated that hoist shafts must not be used to carry ventilation air, hence specialized ventilation shafts are required. Air [ventilation] doors are provided between ventilation shafts and hoist shafts at shaft-bottom car parks. In the past the frequent haulage of materials aggravated air loss due to leakage, but this problem has been greatly reduced since the employment of air baffle systems and similar measures. Although leakage is not as much of a problem with exhaust-type ventilation, exhaust fans do nothing to control the concentration of radon gas evolved in the drifts. Relevant academies, institutes and mines have been brought together in recent years to study the mechanisms by which radon separates out from ore and to find ways of reducing radon concentration, and substantial progress has already been made. Several advanced methods for monitoring air quality and safety are now available at the Ministry of Nuclear Industry, where they are undergoing continual improvement. The installed ventilation capacity per shaft is generally quite high--an average of 40.5 tons of air can be circulated per ton of ore extracted. This is approximately 20 times as much as in coal mines and twice as much as in the Denison uranium mines in Canada. The state specifies that radon concentration in the air at downshaft worksites must not exceed 1×10^{-10} Ci/L and the latent -particle energy from radon decay products must be less tha 4×10^{4} MeV/L. These guidelines can be met for the great majority of worksites by tightening management procedures.

As we have noted above, the drivage-to-extraction ratio in uranium mines is higher than in other kinds of mines, and there has been a tendency for it to increase in recent years. Moreover, the total drivage in [state] capital construction [plan] mines is greater than for other mines. China's uranium mining policy, therefore, has always been to emphasize development of ore extraction and drivage simultaneously, with drivage taking first priority. Moreover, the improvement of tunneling techniques has been resolutely stressed.

In addition to the equipment generally used for driving horizontal drifts, rock drilling platform-cars bracket-type conveyor trains, rock-loading machines equipped with electric hoes, and conveyor belts are also occasionally employed. A rockloader-conveyor equipped with an electric hoe and a mine car which can be unloaded from either side have just been developed. Suspended cages are used in driving raises, with deep-hole sublevel blasting being used occasionally. Rock drills on ring-type mounts, rock grabbers hydraulically anchored against the walls, and other types of advanced equipment are employed to drive vertical shafts. Laser ranging methods have become popular for mining tunnels extending over long distances. Where conditions permit, concrete sprayings, smooth-surface blasting, anchor bolting, etc., may be employed.

In recent years the single-heading footage of drifts tunneled per month has increased somewhat. The current levels are: for horizontal drifts, generally 40-100 meters, with the highest level 345.8 meters in 1978; for vertical shafts, generally 30-40 meters, with a high of 85.3 meters in 1980; the maximum for inclined shafts was 106.2 meters in 1979. All of these figures approach those typical of general (non-uranium) mines in China.

Some mines are located far from smelting plants, and in some cases the ore must be hauled over long distances by railroad to a regional smelter. In a few mines where the ore is easily sorted and cheap to extract, the ore is first selected for radioactivity before being sent to the smelter.

5. CHEMICAL MINING TECHNIQUES

In 1966 the Ministry of Nuclear Industry began an experimental study of chemical methods for mining uranium. Although this work is not yet beyond the experimental stage, good progress has been made and the situation looks hopeful.

In situ [underground] heap leaching experiments have been conducted in a certain mine. This mine is a gently inclined deposit, 15-25 meters thick, in Mesozoic volcanic rock of low-temperature magma-type formation. The compact, hard glassy rhyolite and rhyoporphyry ores are brittle and easily fractured; their most important uranium ore, uraninite, is readily leached. The ore was mined by shrinkage stoping, after which the ore heap was blasted and the pile was drenched with 1-2 percent dilute sulphuric acid solution. The leached liquid was stored in a concentration tank and pumped out to laboratory for solvent analysis. The metal recovery rate was 73.2 percent and the cost of yellow cake production was appreciably reduced.

The quartzite deposits in the Chenzhou uranium mine contain uranium, both as the simple ore and in the form of scattered, impure deposits. Iron pyrite deposits are associated. Natural leaching of the ores occurs. Down in the mine, the worked-out space remaining after all ore is freed by the shrinkage method is used to house the leaching heap. The low-grade ore is stored up there and is drenched with leaching water for a given period to promote leaching of the metal by bacterial action. The leached liquid collected in a tank at the bottom of the shaft, from which it is pumped out to the surface, where the metal is separated. The heap leaching project has been suspended for quite a few years at this mine, but plans are underway to resurrect the project on a larger scale. Good results have also been obtained from heap leaching experiments at several other mines.

The Hengyang Institute of Uranium Mining has been studying boring methods for extracting uranium for many years. Promising results have recently been obtained at several mining sites, and experiments are currently in progress.

6. ECONOMICS OF MINING

Our mining policy is designed to meet China's economic needs. The main goals are to improve mining technology, to mine ore in an economically more productive way, to improve safety while minimizing environmental damage, and to make optimum use of natural resources. In the past there has been excessive emphasis on the utilization of natural resources and on local needs, while insufficient attention has been paid to the overall economics of mining. One of the lessons to be drawn from past experience is that future technical advances must go hand in hand with economic planning.

One of the first questions that arises from an analysis of a dozen-odd representative mines is the maximum economically acceptable cost of ore smelting. This cost is the main criterion by which production should be regulated. A careful analysis of smelting costs will be essential in any future study of the feasibility of opening new mines or implementing important new technical procedures.

We first introduce the quantity Q (Fig. 1) which represents the amount of metal actually recoverable during a given time period, with allowance for the variability in the quality of the ore deposits, ore dilution, hydrometallurgical recovery rate, and mining and hydrometallurgical processing costs from one mine to another. The limiting factor is the hydrometallurgical smelting cost M in yuan/ton (of metal in the finished product), which varies from mine to mine. M is given by the equation

$$M = 100C/[\alpha(1 - \gamma)\varepsilon]$$

where C [yuan/ton] is the cost per ton of ore for extraction, transportation, and hydrometallurgical processing expenses; α is the geological grade of the ore (percent of uranium content); γ is the rate of reduction of grade of ore caused by ore dilution; and ε is the rate of metal recovery through hydrometallurgy.

In Fig. 2 we have plotted the curve S(Q). The straight line OX represents the gross value of output, i.e., the gross income derived from production (Q times the selling price per ton of metal product). The vertical distance between OX and the curve S(Q) represents the total profit under various conditions. The profit is clearly greatest where the tangent to S(Q) is parallel to OX (i.e., above the point Q_1). However, this point corresponds to a relatively low utilization factor of natural resources (the boundary point X corresponds to 100 percent recovery of metal, while Q_1 corresponds to only 89 percent recovery). We therefore select the point Q_2 in order to achieve high utilization and profit simultaneously. The profit at point Q_2 is equal to 94 percent of the profit at Q_1 while 96 percent of the uranium is utilized. Once the point Q_2 has been chosen, the corresponding value of M_2 can be read off the curve in Fig. 1. This value M_2 gives an upper limit for the hydrometallurgical costs if mining is to be economically feasible.

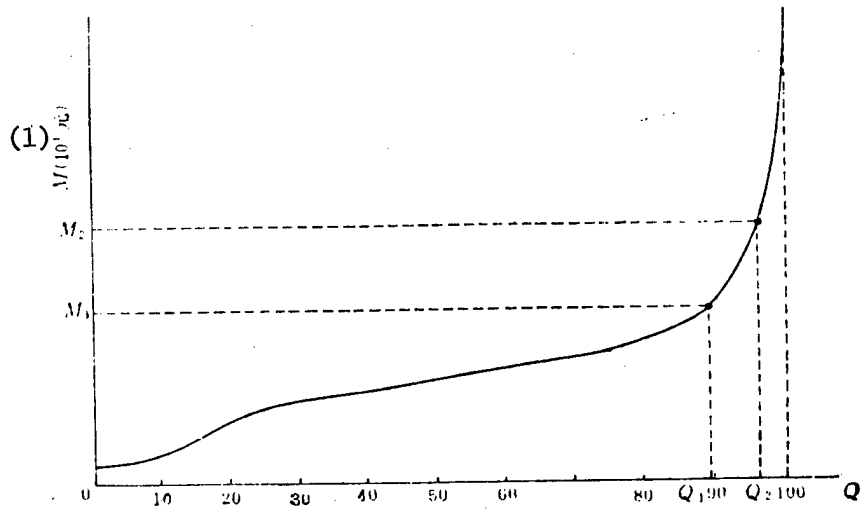

Fig. 1. Amount of Metal Q Obtained During a Given Period of Time for Different Hydrometallurgical Production Costs M.

Key:

1. (10^4 yuan)

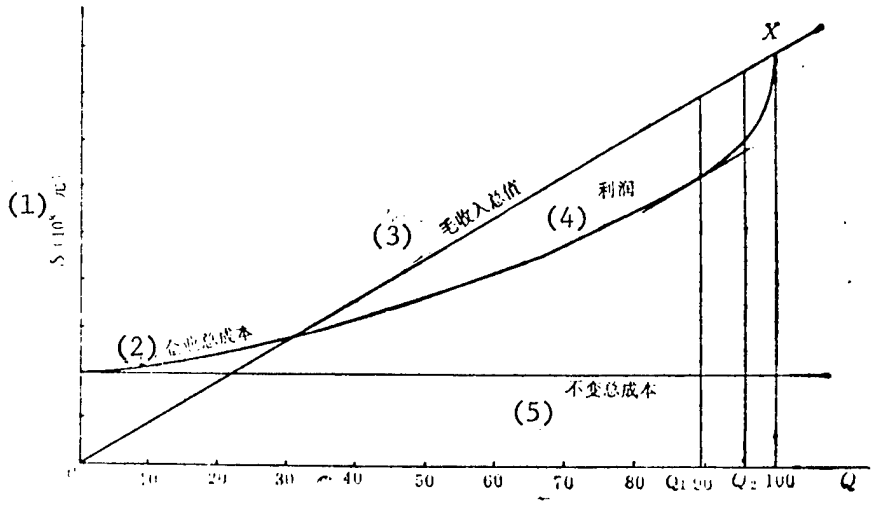

Fig. 2. Plot of Total Expenses S Vs. Percentage Q of Recoverable Metal

Key:

1. (10^8 yuan)
2. Total business expenses
3. Gross income
4. Profits
5. Total fixed costs

7. SOME SUGGESTIONS FOR IMPROVING MINING TECHNIQUES

We list the following suggestions based on the above analysis for improving China's uranium mining technology to reduce costs and derive greater economic benefits.

1. Mining costs are directly influenced by the correct choice of mining method and design and the quality of production management. In the future it will be necessary to devote more attention to study and improve mining methods and to raise production capacity at the workface, quality, the degree of mechanization, and work efficiency. We make the following suggestions germane to these considerations.

(1) Dry-placed fill methods should be done using the most efficient equipment possible. At the same time, ore processing and mining procedures and stope placement must be modified to permit maximum use of available equipment. Where conditions permit, tailings or cement should be used for fill material.

(2) Thin ore strata and veins should be extracted by improved mining methods and techniques to reduce ore dilution. For example, waste-fill methods using cliff debris should be promoted for steeply inclined veins, while techniques for mining long narrow layers should be employed for gently sloping strata.

(3) Where the ore deposits are gently inclined and of medium thickness, we should employ completely open stope methods. We could experiment with roof-reinforcing methods such as roof bolting, possibly supplemented by supporting metal scaffolds. Where necessary, and in mines where conditions are favorable, it may be profitable to study the experience of mines belonging to Finland's Outokumpu Oy Company, which use a single long anchor-bolt to pre-anchor roofs.

(4) In loose ores, we should experiment with downward mining methods which employ cement or concrete slabs for downward fill.

2. Since open-pit mining is safer and cheaper than underground mining, the limits to open-pit mining imposed by a rational stripping-to-ore ratio should be relaxed wherever possible so as to expand the use of open-pit mining. Research on rock mechanics theory should be intensified in order to find methods for controlling landslides and techniques for optimizing side slopes. On the whole, experience indicates that it is worthwhile to use small-scale open-pit techniques to mine the exposed outcroppings of underground deposits.

3. Mining techniques should be simplified at some of the smaller peripheral mining locations. At the pit mouth, only a small amount of movable equipment is required, and this can be transported directly by truck by workers going on or off duty, and costs and investment outlays can be reduced. The experience already gained by Jiangxi Province and elsewhere should be developed further and spread to other areas of China. Where conditions permit, mining profitability may be improved still further by simplifying mining methods and emulating the West in the use of small portable hydrometallurgical plants.

4. At most mines, in the periphery of an ore body of industrial grade, there are commonly associated low-grade ore deposits which are too poor to justify the expense of mining and which are not worthwhile sending to hydrometallurgical processing. In this situation, if heap leaching is feasible, the costs are very low. Moreover, mining costs are also fairly low for low-grade ore mining incidental to the mining of an industrial-grade ore deposit. Economically, it is worthwhile. In this way material formerly wasted can be mined, and resources are utilized more fully. Heap leaching techniques should therefore be promoted vigorously for low-grade ore deposits. Waste rock piles on the surface often contain an appreciable amount of uranium and may also be leached. This will improve the recovery of uranium, while at the same time reducing pollution.

5. In terms of overall administration of the uranium-mining industry, one should naturally give precedence to open up those mines which have richer and more easily mined and processed ore deposits and which promise the greatest economic benefit. In the past, some hydrometallurgical smelters have not been operated at full capacity; this excess capacity should be fully exploited before new smelters are built. As far as is consistent with a good recovery rate for uranium metal, the leaching period should be lengthened in order to reduce the consumption of chemicals and lower smelting costs. When it is necessary to construct a new smelter, efforts should be made to locate the smelter at the mine in order to reduce transportation costs and make the smelted waste products available for filling.

6. Research should also be intensified. In addition to the points raised above, research directed toward a complete solution of the following difficult technical problems should be emphasized:

(1) Techniques are needed for tunneling through and supporting loosely lacked scattered rock formations.

(2) Methods are needed to reduce ore dilution during open-pit mining of thin vein networks.

(3) Methods are required for eliminating water from ore beds prior to mining.

(4) In mines where temperatures are dangerously high, methods must be found either to reduce the temperature and to protect the health of miners from high-temperature, high-humidity environments.

(5) Some of China's proven uranium reserves cannot be recovered at present because they are difficult to process hydrometallurgically or because of high consumption of acids and alkalis. Further experimental studies are needed to find technical breakthroughs which will make it possible to reclaim these reserves.

12617
CSO: 4008/133

SUBSTOICHIOMETRIC DETERMINATION OF CERIUM-141 IN FISSION PRODUCTS

Beijing HE HUAXUE YU FANGSHE HUAXUE [JOURNAL OF NUCLEAR AND RADIOCHEMISTRY] in Chinese Vol 4, No 3, Aug 82 pp 191-193

[Article by Lu Zhaoda [7120 0340 6671], Liu Suqin [0491 4790 3830], and Yu Jiuzhi [0060 0036 1807] of the Northwest Institute of Nuclear Technology]

[Text] I. Introduction

When the isotope inverse-dilution method is used in the measurement of fission products, the errors of analysis mainly come from the measurement of radioactive nuclei and the measurement of the chemical recovery rate of stable isotope nuclei (carrier). Today the measurement technique for radioactive nuclei is greatly improved by advances in equipment and, under certain condition (especially at low carrier level), the measurement error in the chemical recovery of the stable carrier is the main source of error. The authors[1] have measured ^{95}Zr in fission products using the principle of substoichiometric method[2,3]. This method does not require measuring the carrier recovery rate and, since the reaction is with substoichiometric reagents, has a higher selectivity and simplifies the separation procedure. In this paper we report a method for extracting and quantifying ^{141}Ce using substoichiometric di(2-ethyl-hexyl) orthophosphoric acid (HDEHP). The method applies to the measurement of ^{141}Ce, ^{143}Ce or ^{144}Ce in fission products. The relative standard deviation is approximately ± 1.3 percent.

II. Experimental Detail

1. Reagents and equipment

The carrier-less ^{141}Ce solution was extracted from the irradicated concentrated uranium. The purity of HDEHP (analytical purity) was measured by titration to be 97 percent. The Gamma spectrometer was an American Canberra Series-30-1024 channel analyzer and a 3x3 in^2 NaI (TI) doped crystal.

2. Relationship between substoichiometric extraction of Ce(IV) and aqueous phase acidity.

We took 0.4 ml of ^{141}Ce labelled Ce carrier solution (Solution I, 10 mg of Ce per ml), added suitable amount of concentrated nitric acid, 2M $NaBrO_3$ and water

and obtained a 0.5M $NaBrO_3$ solution of the proper acidity. The solution is oxidized for 15 minutes at 40°C and followed by 5 minutes of extraction with 2 ml of 0.01M HDEHP-n-octane. A measured amount of extraction solution was then placed in a cell and the ^{141}Ce radioactivity was measured. Figure 1 shows the relationship between the ^{141}Ce radioactivity in the extraction solution and the aqueous phase acidity. As can be seen, the proper acidity for substoichiometric extraction is 5-7N. The aqueous-phase acidity of the solution used in this work is always 6N HNO_3-0.5M $NaBrO_3$.

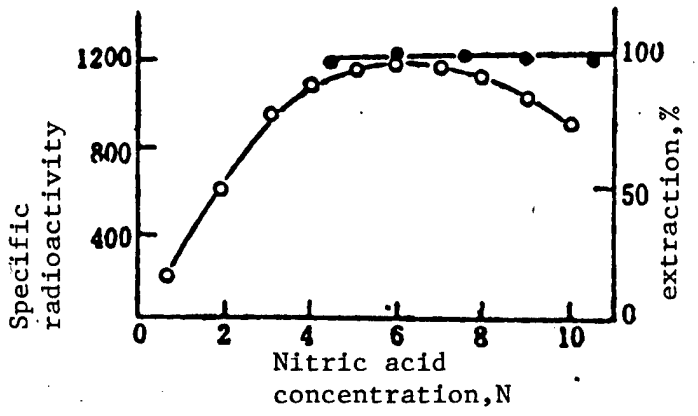

Fig. 1. Effect acidity in extracting Ce(IV) with 0.01M HDEHP-n-octane

o--Substoichiometric HDEHP, this work
o--Excess HDEHP, Ref. 4

3. Reproducibility of substoichiometric extraction

We weighed different amounts of solution I, with a cerium content of 0.4-11 mg, and prepared 2 ml of 6N HNO_3-0.5M $NaBrO_3$ solution. After carrying out the extraction in the manner just described, the extraction solution was weighed and the ^{141}Ce radiation was measured. The specific radioactivity was plotted versus the amount of cerium added, see Fig. 2. The kink point of the curve corresponded to Ce(IV): HDEHP=1 : 2. After this equivalent point, the reproducibility of substoichiometric extraction of cerium was good. Experimental results also showed that the reproducibility was poor when the concentration of the HDEHP-n-octane solution was less than 0.01M.

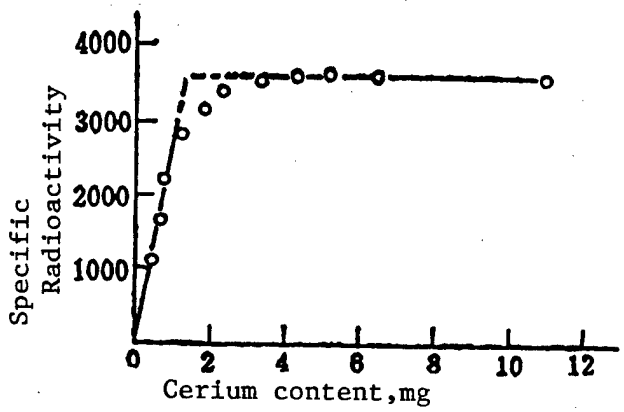

Fig. 2. Reproducibility of Ce(IV) extraction with 0.01M HDEHP-n-octane

4. Relationship between the ^{141}Ce specific radioactivity in the extraction solution and the amount of added ^{141}Ce

We prepared a series of solutions, each solution contained 5.6 mg of cerium but different amounts of ^{141}Ce. The solutions were processed as before and the ^{141}Ce specific radioactivity in the extraction phase was measured. The ^{141}Ce specific radioactivity was plotted against the amount of added ^{141}Ce, a good linear relationship was obtained.

5. Effect of other ions

In a fixed amount of solution I, we added different amounts of various ions. After the extraction, we computed the ^{141}Ce specific radioactivity A. This value was then compared with A_0, the specific radioactivity of extracted ^{141}Ce in the absence of other ions. The results are listed in Table 1.

Table 1. Effects of other ions

Ion	Amount, mg	A/A_0, %	Ion	Amount, mg	A/A_0, %
Ca^{2+}	0.1 1.0	99.6 99.1	La^{3+}	0.1 0.5	100.0 100.0
Sr^{2+}	0.5 2.0	99.7 98.6	Nd^{3+}	0.3 1.0	101.0 101.0
Ba^{2+}	0.1 1.0	100.0 99.6	UO_2^{2+}	0.1 1.0	99.9 99.3
Cd^{2+}	0.1 1.0	98.0 98.8	Mo(Ⅵ)	0.3 1.0	100.1 98.4
Zr(Ⅳ)	0.1 0.3 0.5 1.0	96.0 72.6 15.3 0.6	SO_4^{2-}	0.05N 0.20N 0.50N 2.00N	99.7 101.7 102.0 95.6
Fe^{3+}	0.1 1.0	99.5 101.1	F^-	0.001N 0.015N 0.125N	95.0 91.8 75.8

The results show that Zr(IV) and F^- have a pronounced interfering effect, SO_4^{2-} has no effect when its concentration is less than 0.5N. All other ions have no effect in the range of the present experiment.

6. Analysis procedure for ^{141}Ce in fission products

By accurately adding approximately 5 mg of cerium carrier solution and Mo, Zr and La carrier solutions to the fission product solution sample, we prepared 5 ml of 6N HNO_3-1 percent H_2O_2 solution. Using an equal volume of 0.05M PMBP-xylene solution, we conducted 5 minutes of extraction. The organic phase (containing zirconium) was discarded. The aqueous phase was converted into 5 ml of 7.5N HNO_3-0.5M $NaBrO_3$ solution. It was then oxidized for 15 minutes at 40°C, extracted for 5 minutes with an equal volume of 0.2M HDEHP-n-octane solution. The organic phase was washed twice with 7.5N HNO_3-0.5M $NaBrO_3$ and then back-extracted twice with 5 ml of 7.5N HNO_3-3 percent H_2O_2. The back-extracted solutions were combined and converted into 2 ml of 6N HNO_3-0.5M $NaBrO_3$ solution. After 15 minutes of oxidation at 40°C, it was extracted for 5 minutes with 2 ml of 0.01M HDEHP-n-octane solution. The extracted phase was accurately weighed, placed in a source cell and the ^{141}Ce radiation was measured.

We accurately weighed the carrier-less ^{141}Ce standard solution of known radioactivity, proceeded as above, and computed the value of K to be 6.87 (1 ±0.9 percent). The details are given in Ref. 1.

The procedure just described has sufficient decontamination effect. Irradiated concentrated uranium, 2 days after its removal from the reactor, was purified with this procedure. Using a Ge(Li) γ-ray spectrograph, radiochemically pure ^{141}Ce was verified, simultaneously coexisting with ^{143}Ce and ^{144}Ce.

III. Discussion

We accurately weighed the fission product solution and determined the amount of ^{141}Ce substoichiometrically following the above procedure. The relative standard deviation of 8 measurements was ±1.3 percent and the absolute value also agreed with results obtained by conventional radiochemistry analysis to within 1 percent. The advantages of the substoichiometric method are its high decontamination factor and the small amount of carrier needed. The substoichiometric method appears particularly advantageous for fission products and neutron activated products such as $^{103,106}Ru$ and ^{192}Ir for which the chemical recovery method suffers very large errors.

REFERENCES

1. Lu Zhaoda, et al., HE HUAXUE YU FANFSHE HUAXUE, 3, 34 (1981).

2. J. Ruzicka and J. Stary, Talanta, 10, 287 (1963).

3. Nobuo Suzuki, Kiyoshi Kudo, Analytical Chemistry (Japan), 21, 532 (1972).

4. I. H. Oureshi, et al., Radiochimica Acta, 12, 107 (1969).

9698
CSO: 4008/35

NEW DIGITAL SIGNATURE, PUBLIC KEY CRYPTOSYSTEM

Beijing TONGXIN XUEBAO [JOURNAL OF CHINA INSTITUTE OF COMMUNICATIONS] in Chinese No 1, 1984 pp 1-6, 7

[Article by Lu Tiecheng [4151 6993 1004], Chengdu Institute of Radio Engineering]

[Text]

I. Introduction

With the rapid development of digital communications, people predict that "electronic mail" will progressively replace traditional written letters. This will require that "electronic mail" be provided with security [such that a third party cannot understand it] and identification [that is a signature]. For this reason, it is necessary to borrow the cryptographic techniques from traditional secure communication. Therefore, traditional cryptographic techniques will progressively expand to commercial applications from exclusive use by the military and foreign relations departments of the government. Besides, with the swift development and broad application of computers, cryptographic techniques are also being used to safeguard the secrecy of important documents and data in computer systems.[1]

There are two points to the principal reason for the difficulty experienced with traditional secure communications systems achieving broad utilization commercially. One is that, before secure communication commences, the key must be transmitted through a special secure channel such as courier or registered mail. Also, with an increase in users of the system, the number of keys required by the system grows ever greater. For example, if a system has n subscribers, $n \cdot (n-1)/2$ keys are required. The second point is that there is no way to resolve disputes between sender and receiver arising from the content of the message. This is because in traditional secure communication, the sender's encryption key and the receiver's decryption key are the same. In this way the receiver has the capability to alter and falsify the content of the document and the sender also has an excuse for denying the content of what he sent.

To solve the above two problems, Diffie and Hellman proposed in 1976 a new concept of a secure communication system using a public key.[2] This new concept was a major breakthrough with reference to the traditional secure communications systems. To realize this new concept, several different proposals have already been made.[2-4] Although the proposal described in Document (Ref 2) solves the

problem of security, it cannot solve the signature problem in the transmission of messages. The security of the system described in Document (Ref 3) is established on the basis of the use of very large integers (such as 730-10,000 bits), and the process of providing the signature is fairly complex. The security of the system shown in Document (Ref 4) is conditional--under certain conditions it can be broken.[5]

The new public key secure communication plan proposed in this article, insuring as it does the security of the content of the communication's content, can work for both the dual-user mode and the multiple-user mode. It not only makes the complete system easy to implement, but also can automatically signal a breach of the secret key. Therefore, the plan's operation can suffer no damage whatsoever from partial exposure of the secret key.

II. The Mathematical Basis of the New Plan

The power remainder function in number theory is the basic encryption and decryption function of the new plan. Its principal characteristics are briefly summarized below.[5,6]

For ease of writing, this article has adopted from Document (Ref 7) the symbol $\langle x \rangle$ to indicate the remainder. It represents the remainder from the division of an arbitrary integer x by a positive interger M. Thus $0 \leqslant \langle x \rangle_M < M$.

The definition of the power remainder function is: if

$$\langle x^E \rangle_M = C_x \tag{1}$$

has a solution, C_x would be called the E (secondary) remainder of modulus M and the function shown in Formula (1) is called the power remainder function. In this article [we] select modulus $M = P \cdot Q$, P and Q being different large prime numbers. It is also given that $1 \leqslant x \leqslant M-1$.

If $(E, \phi(M)) = 1$ (that is E and $\phi(M)$ are both prime, the symbol $\phi(M)$ is termed the Euler Function; it expresses the unit [position] number of a positive integer not greater than M and mutually prime with M), the change from x to C_x in Formula (1) is a one-to-one mapping.

If D is the multiplicative inverse of E modulus $\phi(M)$

$$\langle E \cdot D \rangle_{\phi(M)} = 1 \tag{2}$$

$$\text{then} \quad \langle C_x^D \rangle_M = \langle (\langle x^E \rangle_M)^D \rangle_M = x \tag{3}$$

If $\ell = [\phi(P), \phi(Q)]$ expresses the lowest common multiple of $\phi(P)$ and $\phi(Q)$,

$$\text{then} \quad \langle x^{K\ell+1} \rangle_M = x \tag{4}$$

K in the formula is an arbitrary positive integer.

With reference to the power remainder function, the following commutative law appears to have been established

$$<(<x^{E}>_{M})^{D}>_{M} = <(<x^{D}>_{M})^{E}>_{M} \quad (5)$$

Formula (1) and Formula (3) may be used as a pair of encryption-decryption functions. At this time, x is the original message (or block) expressed by a positive integer, E and M are the encryption parameters, D and M are the decryption parameters, and C_X is the encrypted version. If the conversion sequence of the left-hand side of Formula (5) is followed, a public-key encryption-decryption conversion may be established, and, following the conversion sequence of the right-hand side of Formula (5), a signature-and-signature translation conversion may be established.

The power remainder function has excellent cryptographic unidirectional characteristics, therefore gaining important application in cryptography. This type of characteristic may be summarized as follows:

If x, E and M are known, C_X can be calculated very easily according to Formula (1) (the sender's encryption conversion); if C_X, D and M (or E, P and Q) are known, x can be recovered very easily according to Formula 3 (receiver's decryption conversion); if C_X, E and M are known while D (or P and Q) is not, the calculation of x becomes extremely difficult; or, if x, C_X, P and Q are known, the calculation of D would also be extremely difficult (the interceptor's cryptosystem-breaking conversion); the selection, calculation, and changing of system encryption and decryption parameters M, E and D are very easy (user parameter design).

III. The Operational Theory of the New Plan

1. The Basic Theory of Secure Communications Using a Public Key and Digital Signatures

The basic idea in secure communication systems using a public key is to separate the encryption key from the decryption key. The new plan described in this article was developed on the basis of the RSA system.[4] As is the case with the RSA system, it uses the power remainder function as the basic conversion function for encryption-decryption and signature-signature translation. Therefore, it retains the advantage of the RSA system--easy implementation of encryption-decryption and digital signature. In the new plan, each user has his own special pair of public keys E and M for encryption and secret keys D and M for decryption. Each user registers his public key for encryption along with his name and address in the public system users public key book (similar to a telephone directory), safeguarding the security of the secret key D.

Should user A wish to transmit message K securely to user B, he, A, would carry out the encryption conversion of K using the public key of B, then B would use his own secret key to decrypt, recovering K. Should A wish to transmit message K, with his "signature" appended, to B, A would first use his own secret key to convert K, getting a copy with his signature, and then use B's public key to encrypt it, then B would first use his own secret key to decrypt, getting a copy with signature, and then use A's public key to translate the signature to get the original message K.

Using the above idea avoids the trouble of transmitting secret keys through special secure communication channels before having secure communications. It also greatly reduces the number of secret keys in multiple-user secure systems. At the same time it also solves the digital signature problem with the transmission of messages.

The principal distinction between the new plan and the RSA system lies in the addition of an exchange process in message conversion between the sender and the receiver. This enables both the sender and receiver to use the random index encryption conversion to conceal the encryption conversion applied to the transmitted message by the system's public key, thus eliminating the possibility of the enemy's using the special periodicity of the power residue function to break the cryptosystem,[5] and making the security of the new plan vastly superior to the RSA system. At the same time, as a result of the addition of a message exchange between the sender and the receiver in the new plan, the system has the capability of realizing whether the secret key has been revealed to the enemy and whether an interceptor has been introduced into the secure communication process. Therefore, the operation of the entire system would not be harmed by the revealing of the secret key of a portion of it, further raising the level of security and secrecy of the system.

2. Design of Plan Parameters and Conversion Process for Secure Messages

The new plan uses the power residue function described in Formula (1) for public key encryption-decryption conversion, signature-signature translation conversion, and random secret key encryption-decryption. For this reason, each user in the system must produce corresponding encrypt-decrypt key pairs. These key-generation principles are explained below using user A as an example.

User A first randomly selects two different large prime numbers P_{as} and Q_{as} (here the subscript a expresses the parameter selected by user A, and s expresses that said paramter is secret), then, with Formula (6) through Formula (9), secret key D_{as}, and public keys E_{ap} and M_{ap} are produced (Subscript p indicates that said parameter may be made public)

$$M_{ap} = P_{as} \cdot Q_{as} \tag{6}$$

$$(D_{as},\ \phi(M_{ap})) = 1 \tag{7}$$

$$D \neq K[\phi(P_{as}),\ \phi(Q_{as})] + 1 \tag{8}$$

$$\langle E_{ap} \cdot D_{as} \rangle_{\phi(M_{ap})} = 1 \tag{9}$$

In the formulae, K is an arbitrary positive integer. In Formula (6) through Formula (9), a certain subscript has been added to the two large prime numbers P and Q, modulus M and encryption and decryption indices E and D to show that these parameters belong to user A (subscript a), are secret (subscript s) or are public (subscript p). Therefore, these symbols conform with the corresponding symbols in Formula (1) through Formula (5).

Formula (6) indicates that this plan has adopted the compound number M_{ap} as its modulus, permitting the enemy no way of breaking secret key D_{as} using public keys E_{ap} and M_{ap}. This is because mathematically it is easy to find two large

prime numbers P_{as} and Q_{as}, but when M_{ap} is sufficiently large, determining the various prime factors of M_{ap} is extremely difficult.[4]

Formula (7) insures that decryption conversions according to Formula (3) (or encryption conversions according to Formula (1)) are conversions with a one-to-one correspondence. The requirements of Formula (7) and Formula (2) are completely equivalent.

Formula (8) insures that a conversion such as that expressed in Formula (4) does not appear. The development of this restriction is absolutely necessary when using a computer to select encryption indices automatically.

Formula (9) insures that encryption key E_{ap} and decryption key D_{as} are a pair of multiplicative inverses using $\phi(M_{ap})$ as their modulus, thus assuring that Formula (1) and Formula (3) are a pair of reciprocal conversions.

E_{ap} and M_{ap} are used as the public keys of user A, while D_{as}, P_{as}, and Q_{as} are the secret keys of user A.

By the same logic, user B produces his own secret keys D_{bs}, P_{bs}, and Q_{bs} as well as public keys E_{bp} and M_{bp}.

Let us assume that user A wishes to transmit to user B over a common unsecured communication channel a digital message K bearing his signature (or a random key). In accordance with the principles shown in Formula (6) through Formula (9), user A first produces a set of random encryption-decryption keys P_s, Q_s, M_s, E_s and D_s. This set of parameter values is only used for this communication. For the next communication, another set of parameter values must be randomly selected.

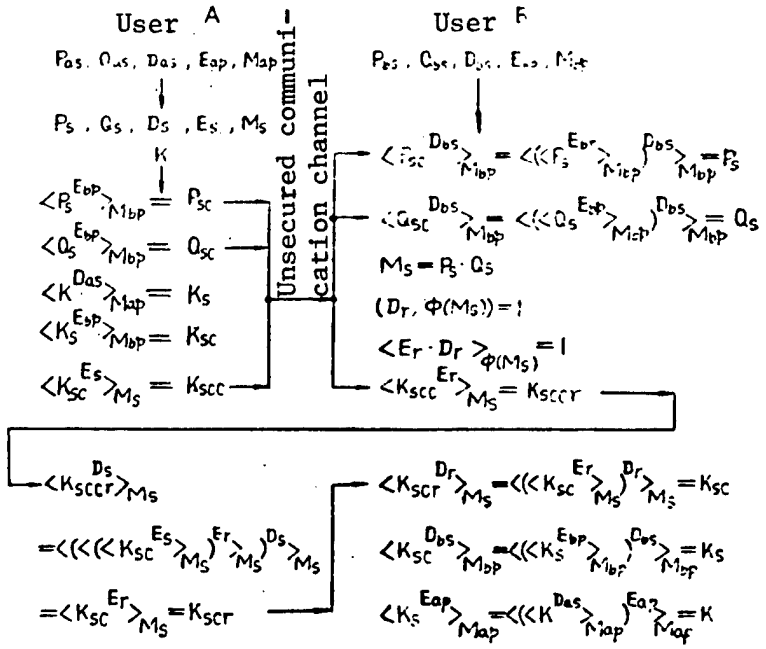

The complete process for transmission of message K is shown in Figure 1. User A carries out the encryption conversion of random prime numbers P_s and Q_s using B's public keys E_{bp} abd M_{bp} according to Formula (1), getting P_{sc} and Q_{sc}. P_{sc} and Q_{sc} are transmitted over an unsecured communication channel to B. Using his own secret keys D_{bs} and M_{bp} according to Formula (3), B carries out the decryption conversion, recovering P_s and Q_s. After this, using P_s and Q_s according to Formula (6) to Formula (9), the receiver's random encryption-decryption keys E_r, D_r, and M_s are produced. To transmit K, A first uses his own secret keys D_{as} and M_{ap} according to Formula (1) to convert K, deriving K_s. With K_s dependent upon message K and also dependent upon user A's secret key D_{as}, K_s is termed the signed version. Next, using B's public keys E_{bp} and M_{bp}, K_s is converted according to Formula (1), deriving K_{sc}. Finally, A's random encryption parameters E_s and M_s are again used to carry out the encryption conversion of K_{sc}, deriving K_{scc}. K_{scc} is transmitted to B over an unsecured communication channel. At first B does not carry out the decryption conversion of K_{scc}, but uses E_r and M_s in accordance with Formula (1) to carry out the receiver's random encryption conversion, deriving K_{sccr}. K_{sccr} is sent back to A over an ordinary communication channel. A uses his random decryption keys D_s and M_s to carry out the decryption conversion of K_{sccr} according to Formula (3), taking the sender's random encryption, deriving K_{scr}. K_{scr} is again sent back to B. B uses D_r and M_s to remove the random encryption of the message by the receiver, uses D_{bs} and M_{bp} to derive the signed version K_s, and again uses the sender's public keys E_{ap} and M_{ap} to recover message K.

3. Identification and Signature

From the above it can be seen that only legitimate receivers (such as B) are able to exchange messages with the sender, from there derive P_s and Q_s, and further derive message K, because only B knows D_{bs}.

In the same manner, only a legitimate sender (such as A) can exchange messages with the receiver (such as B), because B derives K from K_s using E_{ap} and M_{ap}, and only A knows D_{as} which corresponds with E_{ap}.

Obviously the receiver has no way of falsifying or tampering with the version-pair K and K_s, because he does not know D_{as}. In the same manner, neither does the sender have any way to deny that K was transmitted by him, because the receiver has at the same time retained message K and its signature form K_s.

IV. Calculation Methods and Examples

Several typical calculation methods used during the implementation process of this plan are briefly summarized below:

1. The Search for Large Prime Numbers. This plan uses the Monte Carlo Test Method[8,9] to search for large prime numbers, the greatest advantage of this method being its high speed.

2. Seeking a Solution for the Power Remainder. As the search for a solution for the power remainder is an encryption-decryption conversion as well as a requirement for signature-signature translation conversion, it is a basic component of the search process for large prime numbers. To solve for the power

remainder, this plan has adopted the calculating method of repetitive squaring and multiplying of exponents to derive a modulus.[5,10]

3. Selection of Secret Key D. To prevent (the cryptosystem) being broken by the direct search method, a sufficiently large D must be selected. To insure that D_s and $\phi(M_s)$ are mutually prime, the selection of a prime number greater than max (P_s, Q_s) to be D_s is proposed. The method of selecting D_{as}, D_{bs} and so on should be identical to the selection of D_s.

4. Seeking the Solution of Encryption Key E. Encryption key E and decryption key D constitute a pair of multiplicative inverses having $\phi(M)$ as their modulus. This plan uses an expanded Euclidean algorithm to derive various encryption keys.[10]

Figure 2 provides an example of user A transmitting a digital message (or random key) K = 1234567 to user B. It is an output document [file] of a FORTRAN program which simulates the operation of this system.

User A's public key encryption-decryption parameters

P_{as} = 3457 Q_{as} = 2347
D_{as} = 234571 E_{ap} = 4611427
M_{ap} = 8113579

User B's public key encryption-decryption parameters

P_{bs} = 797 Q_{bs} = 12347
D_{bs} = 987659 E_{bp} = 5660347
M_{bp} = 9840559

Sender (A)'s random encryption-decryption parameters and converted message

P_s = 5431 Q_s = 991
D_s = 456791 E_s = 2713511
M_s = 5382121 K = 1234567
P_{sc} = 4739762 Q_{sc} = 2508731
K_s = 5116799 K_{sc} = 2864652
K_{scc} = 626873

Receiver (B)'s converted message (a stroke is added to express it as is the case with A)

P'_s = 5431 Q'_s = 991
E_r = 345679 D_r = 409819
K_{sccr} = 3180012

[continued]

Key of Sender (A) after removal of random encryption

$$K_{scr} = 4406633$$

Key of Receiver (B) after removal of random encryption (a stroke is added to express it as with A)

$$K'_{sc} = 2864652 \qquad K'_{s} = 5116799$$

$$K' = 1234567$$

Figure 2. Example of the Conversion and Exchange of Messages Between Sender and Receiver

V. The Security of the New Plan

The key to the security of the new plan lies in allowing the interceptor no way to break the transmitted secure message K. As can be seen from Figure 1, K has undergone eight power remainder conversions as shown in Formula (10).

$$<(<(<(<(<(<(<(<K^{D_a}>_{M_a})^{E_b}>_{M_b})^{E_s}>_{M_s})^{E_r}>_{M_s})^{D_s}>_{M_s})^{D_r}>_{M_s})^{D_b}>_{M_b})^{E_a}>_{M_a} = K \qquad (10)$$

The most information that an interceptor can acquire includes the public keys E_{ap}, M_{ap}, E_{bp}, and M_{bp} as well as P_{sc}, Q_{sc}, K_{scc}, K_{sccr} and K_{scr} which have been transmitted over an unsecured communication channel. In fact, the interceptor has no way of breaking [the system] and deriving the secret message K from the above information.

If an interceptor wishes to break [the system] and derive the message K, he must first break [the system] and derive random prime numbers P_s and Q_s. It can be known from Figure 1 that breaking for P_s and Q_s is just as difficult as breaking the United States RSA system.[4] Speaking with reference to the new plan, even in the event that an interceptor has already acquired P_s and Q_s, he still has no way of breaking the message K.

Until now the best method of breaking the RSA system has been to utilize the periodicity of the pwer remainder function.[5] It can be seen from Figure 1 that, in the new plan, signals K_{scc}, K_{sccr} and K_{scr} which include message K have all been subjected to the power remainder conversion with random exponents, which effectively conceals the encryption conversion by the public key, so that the interceptor has no way to take advantage of the periodicity of the power remainder function, making the new plan even better with respect to security than the famous RSA system.

It can be known from detailed study of the conversion and transmission process of message K shown in Figure 1 that, assuming the interceptor has already broken P_s and Q_s, the most likely way to break K is to solve for E_s in the following equation:

$$\langle K_{scr}{}^{E_s} \rangle_{M_s} = K_{sccr} \tag{11}$$

further deriving K_{sc}, and then use the method of breaking the RSA system to acquire K. References (2) and (11) point out that seeking a solution for logarithms in a limited domain is extremely difficult. On the basis of this, the secure communication system with two types of public keys proposed in References (2) and (3) was established. From studying Formula (11) it can be known that to find the single solution of E_s is even more difficult than calculating a logarithm in a limited domain, because in Formula (11) modulus M_s is a compound number, and there is no unique solution of E_s. This shows that the security of the new plan will be stronger than the Diffie-Hellman plan[2] and the Merkle-Hellman plan.[3]

In the new plan, should even the secret key such as D_{bs} have been revealed to the interceptor, the system has the capability of discovering this condition. This is because, should an interceptor wish to acquire message K, he would have to masquerade as user B to exchange messages with the sender, and, once such a condition occurs, the sender will receive two (or more than two) answering signals, and will then be able to detemine that there is an unauthorized party participating in the exchange of messages. At this time the sender would immediately suspend the message exchange process and notify the receiver to change his public key and corresponding secret key immediately. Therefore, even if the interceptor should through some means steal many users' secret keys, he would still have no way to disrupt the normal operation of this system.

The principal parameters P_s, Q_s, E_s, D_s, E_r, and D_r (including K itself as well, if K is a key) for transmitting message K all possess a special characteristic of one-time use, that is, all such parameters used in each communication change is random fashion. Obviously the security of such systems will be better than that of systems of which the parameters remain stable and unchanged for a relatively long period.

From the above analysis it can be concluded that the new plan has excellent security.

VI. Conclusion

This article has proposed a type of new plan for secure communications with a public key. This plan utilizes a common unsecured communication channel to provide reliable secure communications and digital signatures. The operation of the entire plan has already been proved and crosschecked by computer, showing that the plan is definitely feasible. The discussion shows that the security of the new plan is higher than that of the RSA system proposed by the Massachusetts Institute of Technology in the United States in 1978 as well as the Diffie-Hellman plan proposed by the Stanford University in the United States in 1976. With respect to ease of implementation of signatures, it is superior to the Merkle-Hellman plan proposed by Stanford University in 1978.

Although this article proves that the new plan is totally secure, the quantitative relationship between security and the length of parameter words requires further detailed investigation.

This research was carried out under the direction of Professor J.K. Wolf of the University of Massachusetts in the United States with the support of Professors L.E. Franks and F.S. Hill. Heartfelt thanks are sincerely extended to Professors Yang Hongquan [7122 7703 6898] and Fan Changxin [2868 2490 0207] who reviewed this article and provided valuable comments.

REFERENCES

1. Diffie, W. and Hellman, M.E., "Privacy and Authentication: An Introduction to Cryptography," PROCEEDINGS OF THE IEEE, Vol 67 No 3, March 1979 pp 397-427.

2. Diffie, W. and Hellman, M.E., "New Direction in Cryptography," IEEE TRANS. INFORM. THEORY, November 1976 pp 644-654.

3. Merkle, R.C. and Hellman, M.E., "Hiding Information and Signatures in Trap Door Knapsacks," IEEE TRANS. INFORM. THEORY, September 1978 pp 525-530.

4. Rivest, R.L., Shamir, A. and Adleman, L., "A Method for Obtaining Digital Signature and Public Key Cryptosystems," COMMUNICATIONS OF THE ACM, February 1978 pp 120-126.

5. Lu Tiecheng, "The Basic Characteristics of Power Residue Functions and Their Application in Secure Communication Systems," TONGXIN XUEBAO [JOURNAL OF CHINA INSTITUTE OF COMMUNICATIONS], publication pending.

6. Niven, I. and Zuckerman, H.S., "An Introduction to the Theory of Numbers," Wiley, New York, 1972.

7. McClellan, J.H. and Rader, C.M., "Number Theory in Digital Signal Processing," Prentice-Hall, Inc., 1979.

8. Solovay, R. and Strassen, V., "A Fast Monte Carlo Test for Primarity, SIAM J. COMPUTING, March 1977 pp 84-85.

9. Lu Tiecheng, "A FORTRAN Program for Rapidly Finding a Large Prime Number," Chengdu Institute of Radio Engineering, Issue 3, 1983.

10. Knuth, D.E., "The Art of Computer Programming Vol 2: Seminumerical Algorithms," Addison-Wesley, Reading, Mass., 1969.

11. Pohlig, S.C. and Hellman, M.E., "An Improved Algorithm for Computing Logarithm Over GF(P) and Its Cryptographic Significance," IEEE TRANS. ON INFORM. THEORY, January 1978 pp 106-110. (Received 6 September 1982)

8174
CSO: 4008/198

ANISOTROPIC STRENGTH PROPERTIES OF ARGILLACEOUS SILTSTONE STUDIED

Nanjing YANTU GONGCHENG XUEBAO in Chinese Vol 6 No 1, Jan 84 pp 32-37

[Article by Zhao Wenrui [6392 2429 3843] of the Northwest Institute of Nuclear Technology: "Strength Properties of Anisotropic Rock of an Argillaceous Siltstone"]

[Text] Abstract

In this paper the strength properties of anisotropic rocks have been measured for an argillaceous siltstone from a location in China. The ultimate strengths for different orientations relative to the stratification planes were obtained by conducting uniaxial compression test, Brazilian tensile test and double shear test for a series of different angles between the applied stress and the stratification planes. The experimental results show that the weak planes of foliated rocks has a marked effect on the ultimate strength of the rock. We therefore believe that it is necessary to take into account the anisotropic properties of foliated rocks as one of the important factors in the testing of the ultimate strength of rocks.

I. Introduction

Although the anisotropic mechanical properties of rocks have been studied since the 1960's, rocks and rock bodies have often been treated as isotropic media in rock engineering design and research. Such simplifications are permissible in most cases, but the anisotropic mechanical properties of rocks must be considered in some other cases such as sedimentation rocks and metamorphic rocks with pronounced anisotropy. Although a number of researchers have investigated the anisotropy of rocks in recent years, but most of the studies are on the metamorphic anisotropy and not the anisotropy of strength. This is probably because the stress conditions encountered in engineering design have not reached the yield strength of rocks.[1]

The shock wave pressure experienced by rocks surrounding the explosion chamber of underground explosions (including nuclear explosions and underground excavation) far exceeds the yield strength of rocks. At some distance away where the shock wave pressure is lower than the yield strength of the rock the deformation is elastic. The anisotropic elastic and strength characteristics in some rocks may lead to spherical asymmetry in the energy attenuation of the shock waves and in the damage of the rocks. The anisotropic strength and elastic characteristics are therefore important topics in the study of rock mechanics when underground explosions are involved.

II. Anisotropy and Classification of Rocks

The anisotropy of rocks is determined mainly by the material composition and the formation process. For example, the orientation of strip and wafer-shaped crystalline minerals, the foliation of metamorphic rock and the weak planes in the laminate of sedimentation rocks may all lead to anisotropic characteristics.

The rock anisotropy can generally be divided into the transverse isotropy and the orthogonal anisotropy.[2] Figure 1 shows a transversely isotropic material in the XOY plane, the mechanical parameters are invariant with respect to direction. This plane is called an isotropy plane. The Z axis is an axis of rotational symmetry. The mechanical properties along the Z direction are different from those in the XOY plane. Such a material is called a transversely isotropic medium. In an orthogonally anisotropic material, three mutually orthogonal elastic symmetry planes can be found for any point in the body, such as the planes 1, 2 and 3 shown in Fig. 2. The normal directions of the elastic symmetry planes (i.e., the X, Y and Z directions) are called the principal directions. A material with such a mutually orthogonal set of elastic symmetry planes is called on orthogonal anisotropic medium.

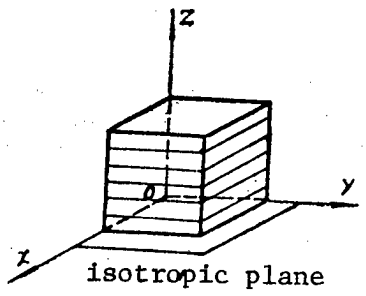

Fig. 1. Transversely isotropic material

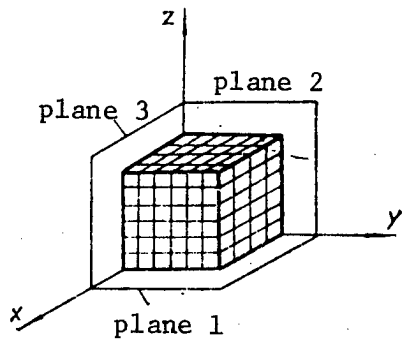

Fig. 2. Orthogonal anisotropic material

III. Site Geology and Petrological Characteristics of the Specimens

The exposed stratum of the sample collecting site is a greyish purple siltstone of the Devonian period in the late Paleozoic era. The lithographic direction runs east and west and tilts toward the south at an angle of 45-60°. Having experienced mild local metamorphic action, such oceanic sedimentation strata usually have uneven laminates with a thickness of 2-5 mm and the laminate bonding is intimate. They usually show stratified color bands of greyish purple and earth tone yellow or greyish purple and light grey or greyish black. The consistency of the rock is dense and hard. The specific volume is 2.73 g/cm^3 and the specific gravity is 2.80. The porosity percentage is 2.5. Microscopic observations reveal that the principal mineral component of the rock is quartz (approximately 70 percent) followed by feldspar and small amount of other minerals. The rocks have a medium degree of round-off and the grain size is 0.01-0.03 mm. The adhesive in the rock is a carbonate and argillaceous minerals and the adhesive is along the basal planes. After mild local metamorphic changes, the carbonate has recrystallized into grains of calcite with a size of 0.01-0.05 mm. Under a microscope, an oriented array of biotite laminates can be seen along the fine stratified surface. After core and wafer observation, the rock is given the name greyish purple metamorphic argillaceous siltstone.

In the study of lithographic anisotropy, such rocks with a pronounced laminated structure are often treated as transversely isotropic media. The laminates are the planes of isotropy and the normal to the layers is the axis of rotational symmetry (the Z-axis).

IV. Sample Preparation

The experimental specimens are taken from drilled cores 50m below the earth surface. Due to the small core size, the compression and tensile specimens are only 5x5x5 cm^3 and the shear specimens are 3x3x7 cm^3 square posts. Compression specimens are fabricated with the angle between the load direction and the laminate equal to 0°, 15°, 30°, 45°, 75° and 90°. For the tensile specimen, the angles are 0°, 30°, 60° and 90°. The shear specimens are made to have an angle of 0°, 15°, 45° and 90° between the shear direction and the laminate plane. Three samples are made for each angle and each strength test. Samples without cracks or at least without through cracks to the naked eyes are used in the tests to avoid the pronounced effects of cracks on the mechanical properties. For the sake of briefty, we use β to represent the angle between the applied force and the laminate plane.

V. Test Results

The uniaxial compression tests are conducted on a 200-ton press using the conventional method.

The tensile tests are conducted using the Brazilian split tensile method. Two circular cylinders are placed against two opposite faces of the cube and the load is applied through the cylinders. The experimental arrangement and the force diagram are shown in Fig. 3.

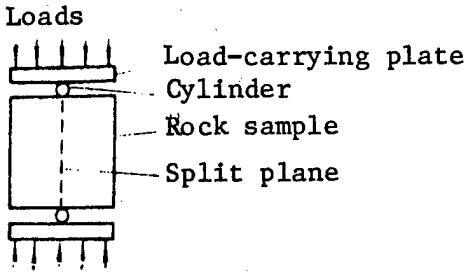

Fig. 3. Schematic diagram of the split method

The shear strength is measured in a double shear test. All the test results are summarized in Table 1. Figures 4-6 show the variations of strength as a function of β.

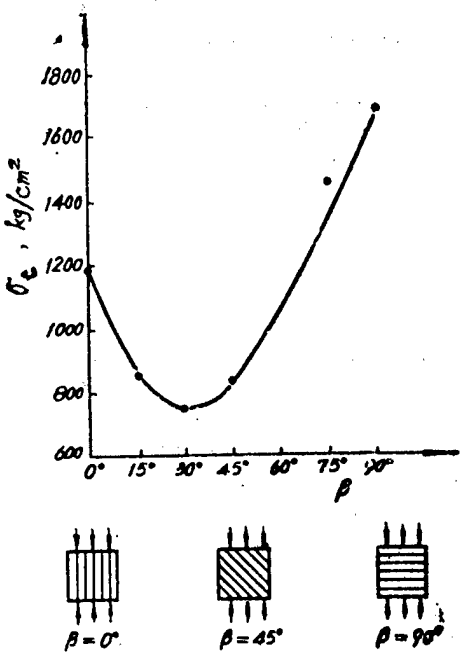

Fig.4. Uniaxial compression strength of argillaceous siltstone versus β

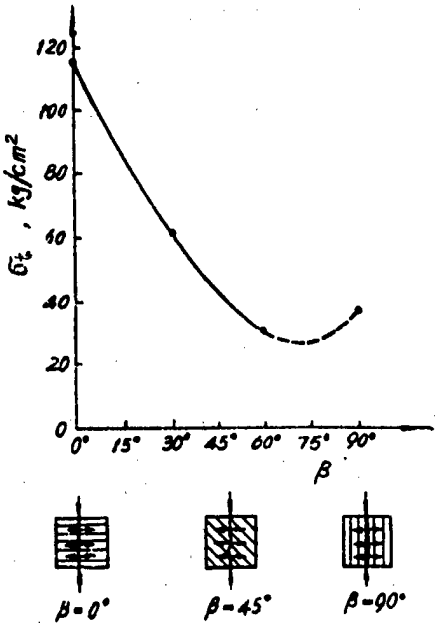

Fig.5. Tensile strength of argillaceous siltstone versus β

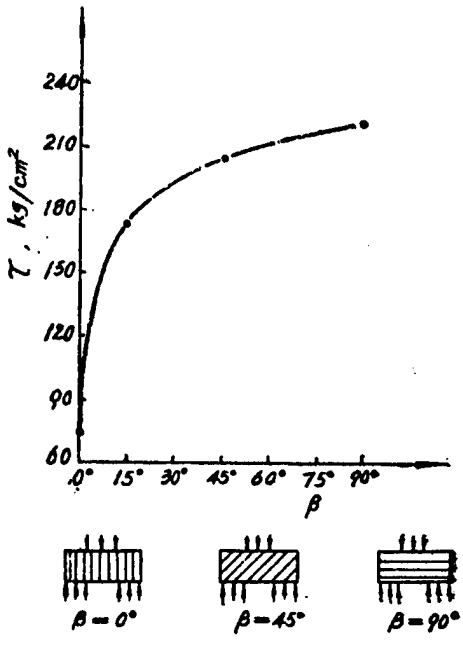

Fig.6. Shear strength of argillaceous siltstone versus β

Table 1. Test results for different angles between the principal stress and the laminate plane

Angle β	Compression limit σ_c (kg/cm^2)		Tensile limit σ_t (kg/cm^2)		Shear limit τ (kg/cm^2)	
	Measured	Average	Measured	Average	Measured	Average
0°	922 1502 1137	1187	119 103 127	116	80 67	74
15°	888 723 917	843	/	/	192 149 183	175
30°	843 630 792	755	35 81 71	62	/	/
45°	960 646 1044	883	/	/	146 229 244	206
60°	/	/	20 31 44	32	/	/
75°	1298 1204 1877	1460	/	/	/	/
90°	1698 1502 1886	1695	44 38 32	38	266 248 152	222

As can be seen from Table 1, the uniaxial compression strength of the finely laminated siltstone changes with β. When the applied force makes an angle of 30° with the plane, the compression strength is a minimum: σ_c = 755 kg/cm^2. When the load is applied parallel to the plane (β = 0°), the compression strength is less than that for β = 90° and greater than that for β = 30°. The maximum strength is 2.25 times the minimum strength.

The compression-versis-β curve has the shape of a parabola, as shown in Fig. 4.

Figure 5 shows the results of the Brazilian tensile tests on the argillaceous siltstone. When β = 60-75°, the tensile strength σ_t is a minimum, approximately 30 kg/cm^2. When β = 0°, the tensile strength σ_t has a maximum value of 116 kg/cm^2. The maximum is 3.53 times the minimum. When β = 90°, the value of σ_t is somewhat higher than that at β = 60-75° and the curve has a slight up-turn near the end.

The shear test results in Fig. 6 show that the shear strength τ is a minimum at β = 0° and has a value of about 74 kg/cm^2. As β increases, τ also increases and reaches a maximum value of 222 kg/cm^2 at β = 90°. The maximum is 3 times the minimum.

The mode of fracture of the test specimens also changes with β. For the compression specimen, the failure is a tensile fracture accompanied by shear fracture when β = 0°. For β = 15°, 30° and 45°, the fractures are along the laminate planes. For β = 75°, there are some fractures along the planes and at β = 90° the fracture is the shear type. For the tensile specimens, the facture is basically taking place along the applied stress, but when β is 30° or 60°, the fractured surface is step-like because of the influence of the laminates. For the shear specimens, the failure is along the shear plane when β = 0° or 90°. When β is 15° or 45°, the fractured plane is again step-like because of the lamintes.

VI. Discussion

In the uniaxial compression tests of the rock anisotropy, the principal mode of fracture is along a 30° angle from the principal stress axis. When the weak surface of the laminate is at a 30° angle relative to the principal stress, the weak surface is at an orientation most favorable to fracture and the strength of rock is the lowest.* Another mode of fracture in the uniaxial compression test is along the direction of the principal stress. The strength is also low when the laminates are aligned with the stress direction, but higher than the strength when the weak surface is at a 30° angle from the principal stress direction. When the weak surfaces are perpendicular to the principal stress, the weak surfaces have very little effect on the strength and the strength in this configuration is the highest.

---

* Yasuo Mogi, Rock Mechanics and Earthquake, Collection of lectures given in China, 1978.

Some references in the literature often give only the compression strength perpendicular and parallel to the laminates; this is ovbiously not enough. The triple-axis compression tests of shale rock by F. A. Donath,[3] the uniaxial compression tests of schist by G. Barla[4] and our uniaxial compression tests of siltstone have all demonstrated that the strength is lowest when the principal stress axis makes a 30° angle with the weak surface. We, therefore, conclude that, in order to give a complete description of the strength anisotropy of the rock, one must at least give the compression strength for the principal stress perpendicular to the weak surface, parallel to the weak surface and at angle of 30° with the weak surface.

Very little information is available on the Brazilian tensile test of rock anisotropy. In 1972 G. Barla and N. Innau conducted tensile tests on the anisotropy of circular disk specimens of Italian Susa granite gneiss. Their results are similar to our findings: the strength is a maximum when $\beta = 0°$, the strength is a minimum when $\beta = 60\text{-}75°$ and the measured strength at $\beta = 90°$ is slightly greater than the minimum strength. It should be pointed out that the anisotropy of tensile strength of a rock specimen clearly depends on the testing method. For example, the experimental results of direct tensile tests of gneiss made by G. Barla and L. Goffi showed that the minimum strength is at $\beta = 90°$. Evidently more theoretical and experimental efforts are needed to understand the effects of anisotropy on tensile strength.

Here we should point out the difference in fracture situations in a compression test and in a Brazilian tensile test. In a compression test with $\beta = 0°$, the specimens mainly fracture along the laminates, as shown in Fig. 7. In a Brazilian tensile test with $\beta = 90°$, however, the fracture occurs along the laminate in the vicinity of the load surface experiencing the linear concentration of stress. Although the rock specimen fractures along the laminates in both cases, the compression test produces a number of fracture planes and the fracture mechanism is a lateral expansion under an axial load. In the split test, however, the specimen showed only one fracture plane and the mechanism is as follows: the cylinders used in the split test transform the external load into a tensile stress in the interior of the rock and the specimen splits under tension along a load plane with a linear concentration of stress. The fracture mechanisms are different in the two cases and the strength limits are also quite different. The former corresponds to the limit of compression strength and the latter corresponds to the limit of tensile strength.

Fig. 7. Fracture under an uniaxial load

The effect of anisotropy on shear strength has not been reported in the literature. Our results of double shear tests on the argillaceous siltstone showed that the weak surfaces of the rock indeed have a noticeable effect on the shear strength. This conclusion is only preliminary and further investigations are needed.

The author thanks He Zhuqing [6320 5416 7230], Zhao Jingzhen [6392 2417 3791], Tang Rundi [1781 3387 2769] and Wu Guorong [0702 0948 2837] for their participation in the experiments.

References

1. Tao Zhenyu [7118 2182 1342], Rock Mechanics in Hydraulic Engineering, Water Conservancy and Electric Power Publishing Company, 1967 p 13.

2. Hikaru Suzuki, Rock Mechanics and Measurements, Translated by Yang Qizhong [2799 0366 0022], et al., Coal Industry Publishing Company, 1980 pp 230-237.

3. Donath, F. A., Strength Variation and Deformation Behavior in Anisotropic Rock, in "State of Stress in the Earth's Crust," edited by Williamr Judd, 1964 pp 281-298.

4. L. Miller, Rock Mechanics, translated by Li Shiping [2621 0013 1627], et al., Coal Industry Publishing Compnay, 1981 pp 112-142.

9698
CSO: 4008/210

BRIEFS

OVERSEAS SCIENCE INSTRUMENTS EXHIBITION--Chengdu, 25 July (XINHUA)--An exhibition of scientific instruments from Hong Kong and abroad opened today in Chengdu, capital of Sichuan Province. On show are analysing and testing instruments, precision electronic equipment, microcomputers, semi-conductor components and parts, duplicators, microscopes and foamed plastics packaging devices from 12 firms in Hong Kong, the U.S. and Japan. The exhibition, sponsored by the Technical Exchange Center and Scientific Instruments Corporation of Sichuan Province, ends next Tuesday. [Text] [OW252114 Beijing XINHUA in English 1458 GMT 25 Jul 84]

CSO: 4010/124

BRIEFS

DRUG FOR ACUTE RADIATION SICKNESS--"500" is a drug for the prevention and treatment of radiation injury. Research on the synthesis, dosage, effectiveness, toxicity, and metabolism of the drug and tests on humans have shown that this drug can lower the level of the body's reaction to radiation and decrease the rate of chromosome aberration. The prophylactic effects for animals and humans suffering from radiation damage are good and can enhance the effects of other radiation protective agents and therapeutic measures. The production techniques for "500" are advanced, the raw material is domestic, the cost is low, and it has broad applications. [Article by the Academy of Military Medicine Shanghai No 9 Pharmaceutical Factory] [Text] [Beijing JIEFANGJUN YIXUE ZAZHI [MEDICAL JOURNAL OF CHINESE PEOPLE'S LIBERATION ARMY] in Chinese No 3, 20 Jun 84 p 221]

CSO: 4008/372

AUTHOR: HUANG Kezhi [7806 0344 2535]
XUE Mingde [5641 2494 1795]

ORG: Both of the Department of Engineering Mechanics, Qinghua University

TITLE: "A Comparison of Chinese Pressure Vessel Design Regulations on Tubesheets of Heat Exchangers with American Standards of TEMA and Its Verification by Experiments"

SOURCE: Beijing LIXUE XUEBAO [ACTA MECHANICA SINICA] in Chinese No 1, 1984 pp 43-50

TEXT OF ENGLISH ABSTRACT: In this paper, the theoretical bases of the Chinese design formula on tubesheets are summarized and compared with the American standards of the TEMA (Tubular Exchanger Manufacturers Association), which are used by many designers in the world. The experimental results on six tubesheets are given. It is clear that the results obtained by the authors' formula are in much better agreement with those of the experiments. The conclusion is that this method is more reasonable than that of the TEMA.

AUTHOR: SUN Siyuan [1327 1835 6678]
SANG Fengting [2718 7685 0080]
ZHOU Biqian [0719 1801 6692]
et al.

ORG: All of the Dalian Institute of Chemical Physics, Chinese Academy of Sciences

TITLE: "LIF Visualization of Supersonic Chemical Laser Flowfields"

SOURCE: Beijing LIXUE XUEBAO [ACTA MECHANICA SINICA] in Chinese No 1, 1984 pp 92-95

TEXT OF ENGLISH ABSTRACT: By using an improved laser fluorescence (LIF) technique, we have succeeded in displaying the whole flowfield of cw supersonic chemical lasers. A salient feature of this method is its high spatial resolution (< 0.5 mm) in the direction normal to the incident beam, which is difficult to obtain by other methods. Due to the fluorescence quenching at the shock front, distinct shock patterns become observable in the LIF photograph. These are subjected to quantitative data processing to obtain the local Mach numbers. The influence of the trip, i.e., a minute amount of He gas injected transversely into the main flow, on the spreading and mixing of two supersonic gas streams is investigated.

9717
CSO: 4009/110

AUTHOR: PAN Xiaohong [3382 1321 3163]

ORG: None

TITLE: "A Calibration Method for Measuring Hydrophones at Low Frequencies"

SOURCE: Beijing JILIAN XUEBAO [ACTA METROLOGICA SINICA] in Chinese No 2, 1984 p 106

TEXT OF ENGLISH ABSTRACT: This paper proposes a novel calibration method for measuring hydrophones at low frequencies. The measurement of the hydrophones of different types can be calibrated over a wide frequency range with rapid speed and simple equipment. The total uncertainty of the calibration using this method is less than ± 1.0 dB within the frequency range of 5 to 2000 Hz.

9717
CSO: 4009/101

AUTHOR: YANG Mingjiu [2799 2494 0036]
HE Shen [6378 3933]
WANG Fuzhong [3769 4395 1813]
YU Weifu [0060 4850 4395]

ORG: All of China Medical College, Shenyang

TITLE: "Studies on i-RNA Activity Expression by Cell Fusion Technique"

SOURCE: Beijing ZHONGHUA WEISHENGWUXUE HE MIANYIXUE ZAZHI [CHINESE JOURNAL OF MICROBIOLOGY AND IMMUNOLOGY] in Chinese No 2, Apr 84 pp 74-76

TEXT OF ENGLISH ABSTRACT: RNA was extracted from the liver and spleen of both normal (N-RNA) and HeLa cell immunized (i-RNA) rabbits. N-RNA, N-RNA plus a very small amount of HeLa cell antigen (N-RNA + Ag), i-RNA and i-RNA pretreated with RNase, DNase or Pronase were sealed respectively into mouse erythrocyte ghosts by hypo-osmotic dialysis. These ghosts were then fused with myeloma cells by the ghost fusion method under PEG treatment. The above-mentioned RNAs were injected from each ghost into myeloma cells through cell fusion. The fused cells were cultured and the specific antibody against the HeLa cell was detected with ELISA. It was demonstrated that no such antibody was produced by cells injected with N-RNA, N-RNA +Ag, or i-RNA (RNase), but the specific antibody appeared in the supernatant of the culture media 96 hours after injection of i-RNA, i-RNA (Dnase) and i-RNA (Pronase). Continuous cell culture, observation and regular changing of medium revealed that production of the antibody lasted for 2 weeks.

AUTHOR: HUANG Peitang [7806 1014 1016]
XIONG Lingshuang [3574 0407 7208]
MA Qingjun [7456 3237 6874]
et al.

ORG: All of the Institute of Basic Medical Sciences, Academy of Military Medical Services, Beijing

TITLE: "Detecting Expression of Cloning Gene with Minicells"

SOURCE: Beijing ZHONGHUA WEISHENGWUXUE HE MIANYIXUE ZAZHI [CHINESE JOURNAL OF MICROBIOLOGY AND IMMUNOLOGY] in Chinese No 2, Apr 84 pp 98-100

TEXT OF ENGLISH ABSTRACT: E. coli DS410 minicells with and without recombinant plasmids were purified on a 5-25 percent linear sucrose gradient and then labeled with ^{35}S-methionine. The lysate of minicells was separated on 12.5 percent SDS-polyacrylamide gels. The gels were dried and exposed to X-ray film for about one week. The autoradiographs obtained showed that no significant incorporation could be found for the plasmid-free minicells, whereas very dark bands appeared on the autoradiographs of the plasmid-containing minicells. The minicells with pBR322 synthesized four polypeptides being coded for by Tc^r and Ap^r genes. The minicells with pBR325 synthesized five polypeptides, one of which was coded for by Cm^r gene, with the others being identical to those synthesized by the minicells with pBR322. The reports of results from recombinant DNA-containing minicells indicated that not only the vector resistance genes, but also the inserted foreign DNA sequeces could be expressed in minicells.

Our results were quite similar to those published, i.e., minicells can be used to detect the expression of cloning genes, especially foreign genes with unknown functions.

9717
CSO: 4009/104

AUTHOR: WANG Jiao [3763 4109] and TANG Jiahuan [0781 1367 2970]

ORG: 728 Engineering Research and Design Institute

TITLE: "Analysis of Calculated Statistical Mean Temperature of Fuel Rod"

SOURCE: Beijing HE KEXUE YU GONGCHENG [CHINESE JOURNAL OF NUCLEAR SCIENCE AND ENGINEERING] in Chinese Vol 3, No 3, Sep 83 pp 193-201

ABSTRACT: The temperature of a fuel rod is greatly affected by the thermal conductivity across the air gap between the pellets and the zirconium tube. Initially, the positions of the pellets are randomly distributed and the temperature of the fuel rod should be a statistical average. The formulas for the probability of eccentricity of fuel pellets and the statistical mean temperature of the fuel rod were derived and used in the calculation for the 300MW(e) reactor at the 728 Institute. Results indicated that most of the pellets were randomly distributed eccentrically. The maximum temperature of eccentric pellets was found to be lower than that of concentric ones. When the nominal air gap thickness was 85 μm, the statistical average of the maximum temperature was 1.47 percent lower than the concentric value. The maximum temperature of the 728 Institute reactor might differ by 17.4 percent, where the maximum air gap thickness was 110 μm and the minimum was 65 μm. The statistical mean value was 9.14 percent lower than the maximum. The temperature of the fuel rod was a temperature band and the effect of air gap thickness was apparent.

12553
CSO: 4009/33

AUTHORS: BIAN Hongxing [0593 3163 5281], JIA Zhanli [6328 0594 4409], and ZHAO Qingzhen [6392 1987 3791]

ORG: All of Institute of Atomic Energy, Academy of Sciences

TITLE: "Investigation on Loss of Power for a Heavy Water Research Reactor"

SOURCE: Beijing HE KEXUE YU GONGCHENG [CHINESE JOURNAL OF NUCLEAR SCIENCE AND ENGINEERING] in Chinese Vol 3, No 3, Sep 83 pp 202-210

ABSTRACT: The cooling mode involving the use of an auxiliary heavy water pump at 1500 rpm during a loss of power accident of a heavy water research reactor was studied. Both theoretical calculation and experimental measurements were used to determine the surface temperature of a fuel element in order to evaluate the safety and reliability of the cooling system. A simplified model was adopted to establish the steady state and dynamic heat transfer equations. After a loss-of-power accident, heat was primarily generated by the neutron power, fission products decay and actinium series decay. A point reactor model was used to calculate the neutron power. The heat released by fission products was calculated according to the "1978 ANS 5.1" standard as recommended by the American Nuclear Society in 1978. As for the actinium series decay, only U-239 and Np-239 were taken into account. Actual measured hydraulic parameters of the reactor were used in the dynamic calculation. All the computations were done on the TQ-6 computer at the Institute of Atomic Energy using programs in BCY language. Experimentally, nichrome-alumel thermocouples were used as temperature sensors. The time constant for sampling was τ_0 = 23 ms. The surface temperature of the fuel element was measured under a steady state condition, which was found to be in good agreement with the corresponding theoretical value. Finally, a total loss of power experiment was conducted after the reactor had operated continuously for 140 hours at a nominal power of 8,000 kW with 56 loaded tubes. The auxiliary pump activated after the loss of power was found to sufficiently provide cooling to maintain the surface temperature at below 136.0°C to avoid boiling. Two peaks were found on the temperature-time curve which were explained in detail. The calculated value was slightly higher than, but in good agreement with, the experimental results.

12553
CSO: 4009/33

AUTHORS: XIANG Fengduo [7309 7685 6995], and Wang Meijun [3769 3270 0689]

ORG: XIANG of Wenzhou Teachers' College, WANG of Institute of Atomic Energy, Academy of Sciences

TITLE: "Thermal Neutron Spectrum of Zirconium Hydride Moderator"

SOURCE: Beijing HE KEXUE YU GONGCHENG [CHINESE JOURNAL OF NUCLEAR SCIENCE AND ENGINEERING] in Chinese Vol 3, No 3, Sep 83 pp 231-238, 250

ABSTRACT: Zirconium hydride can be used as a good thermal neutron moderator even at very high temperatures. Their interaction is a typical case of incoherent scattering. The scattering cross-section had been experimentally determined previously. An in-depth study of the thermal neutron spectrum was conducted in this work. A multigroup diffusion approximation was used to calculate the thermal neutron spectra in zirconium hydride as well as in a zirconium hydride-water zero-energy device by dividing the energy region below 0.625 eV into 30 groups. The calculation of the scattering nucleus was based on the phonon spectrum and the double differential cross-section formula. The theoretical thermal neutron spectrum in zirconium hydride was found to be similar to that in poisoned water (by boron) where the equivalent absorption cross-section of each hydrogen atom is 0.756. The spectrum was shifted toward higher energy than that in water because the absorption cross-section of zirconium is higher than that of oxygen. The energy spectrum showed fine structures at 0.02, 0.14 and 0.28 eV, corresponding to various effects of the optional and acoustic branches of the phonon spectrum. These fine structures could not be calculated by a simple free hydrogen atom model, or even by the Einstein model. The effects of poison level and temperature were also investigated. Finally, the thermal neutron spectrum of a zirconium hydride-water zero energy device was calculated based on the scattering matrix obtained from the scattering nucleus theory. Good agreement was found between calculated and theoretical results. The same principles were also found to be applicable to other solid moderators.

12553
CSO: 4009/33

AUTHORS: LI Wendan [2621 2429 --?-], CUI Guangyu [1508 1684 7411], ZHANG Lili [1728 5461 7787], WU Aiju [0702 5337 5468] et al

ORG: All of Institute of Atomic Energy, Academy of Sciences

TITLE: "Thermal Diffusivity and Conductivity of Uranium Dioxide at High Temperature"

SOURCE: Beijing HE KEXUE YU GONGCHENG [CHINESE JOURNAL OF NUCLEAR SCIENCE AND ENGINEERING] in Chinese Vol 3, No 3, Sep 83 pp 251-257, 271

ABSTRACT: The thermal diffusivity of uranium dioxide was measured in the temperature range of 573-2773°K by a laser pulse method with 10 nearly stoichiometric samples (theoretical density 96.5 percent). Precautionary measures were taken to ensure the homogeneity of the laser pulse as well as to minimize the heat loss and non-instantaneous pulse effect. The measurements were made in a tantalum tube furnace filled with high purity argon at about 1000 Torr. The temperature of the specimen was measured by a W-Re thermocouple at below 2273°K and a fine focus optical pyrometer at about 2273°K. The thermal diffusivities obtained were corrected for thermal expansion by using the average linear expansion coefficient reported by other workers. Its error was estimated to be $\pm$ 5 percent. Thermal diffusivity data was then used to calculate the thermal conductivity at UO_2. It was found to decrease with increasing temperature at $T < 1673$°K due to heat conduction by phonons. The minimum thermal conductivity was 0.0228 W/cm.K at approximately 2000°K. Then it began to rise with increasing temperature; resulting from heat conduction by thermally activated electrons. The activation energy of electron E_a was found to be 1.2eV. At higher temperatures, the thermal conductivity decreased because of more intense electron scattering due to oxygen vacancy formation. The formation energy of an oxygen vacancy was estimated to be 5.2eV. Finally, an empirical expression for the thermal conductivity throughout the temperature range was determined and its maximum standard deviation was 0.004 W/cm.K. Specimens used in this work were provided by relevant departments of the Ministry of Nuclear Industry.

12553
CSO: 4009/33

AUTHORS: XIONG Xingshan [3574 1840 0810] and LIU Enchong [0491 1869 0339]

ORG: Both of Ministry of Nuclear Industry

TITLE: "Present Mining Technology and Future Development Policy at Chenxian Uranium Mine"

SOURCE: Beijing HE KEXUE YU GONGCHENG [CHINESE JOURNAL OF NUCLEAR SCIENCE AND ENGINEERING] in Chinese Vol 3, No 3, Sep 83 pp 264-271

ABSTRACT: The present mining technology at the Chenxian Uranium mine--one of the oldest uranium mines in China--is described in this paper. The orebody is composed of quartzites embedded in a metamorphic sedimentary deposit. Currently, a horizontal tier backfill method is used, producing 700 tons per day. The ores are first up-graded by radiometric sorting and then treated hydrometallurgically. Each ton of ore consumes 70 kg of sulfuric acid. The leaching rate is 90 percent and the metal recovery rate is 87 percent. It requires 1.25 tons of ore to obtain 1 kg of uranium at a total mining cost of 125 yuan. The amount of hot water produced is 1500 m^3/h and the water temperature is 45-47°C. It is expected to reach 2700-3200 m^3/h at 58°C when the deepest level is mined. In order to overcome these difficulties, four specific policies were proposed. First, working faces will be cooled by refrigeration by a centralized station with a cooling capacity of 10^6 kcal/h. Holes will be drilled to drain the water and improve the environment. Secondly, low-grade ores will be mined together with regular ones. They will be graded to be further processed by radiometric sorting, heap-leaching, or possibly bacterial leaching before undergoing hydrometallurgical treatments. Thirdly, the excavation method will be improved to minimize the drainage costs. Finally, hot water will be widely utilized to reduce the ore costs and save energy.

12553
CSO: 4009/33

AUTHOR: GUAN Xialing [7070 6667 0109]

ORG: Institute of Atomic Energy, Academy of Sciences

TITLE: "Optical Characteristics of the HI-13 Tandem Accelerator"

SOURCE: Beijing HE KEXUE YU GONGCHENG [CHINESE JOURNAL OF NUCLEAR SCIENCE AND ENGINEERING] in Chinese Vol 3, No 3 Sep 83 pp 281-285

ABSTRACT: The beam optical characteristics of the HI-13 tandem accelerator at the Beijing Institute of Atomic Energy were calculated using the "Optics-II" program which was originally used for the XUT tandem accelerator at Padova University in Italy. The HI-13 accelerator is an electrostatic tandem heavy ion accelerator built by HVEV in the United States. At a terminal voltage of 13 MeV, it is capable of producing a 26 MeV proton beam. The acceptance of the double aperture system in the injector was found to be 6.5 mm-mrad$(MeV)^{1/2}$; compatible with that of the main tandem accelerator. Particle beams passing through these apertures could be transported across the stripper without suffering any loss. In the low energy acceleration stage, an inclined electric field was used to suppress electrons and to increase the gradient of the accelerator tube. At m3MeV, the horizontal and vertical acceptance values of a proton beam were 15 and 7 mm.mrad$(MeV)^{1/2}$, respectively. In the high energy acceleration stage, the emittance became larger with increasing particle mass and decreasing terminal voltage. The mass-energy product of the 90° analyzing magnet was 200. The sizes of proton and chlorine ion beams were calculated based on the maximum acceptance. Finally, the pulse time characteristic of the HI-13 accelerator was calculated by the longitudinal transport matrix program. A double-peak waveform of a proton beam was obtained. In summary, the transport efficiency of the injector can reach above 95 percent. However, it is less than 65 percent in the low energy acceleration stage. The high energy accelerator can transport light particles without loss. For heavy particles, the efficiency depends on the type and charge of the particle.

12553
CSO: 4009/33

AUTHOR: WANG Maoquan [3076 5399 3123]
ZHAO Qingchu [6392 2532 0443]

ORG: Both of the Institute of Plasma Physics, Chinese Academy of Sciences, Hefei

TITLE: "The Restraint of the Tearing Modes in Tokamak"

SOURCE: Beijing WULI XUEBAO [ACTA PHYSICA SINICA] in Chinese No 4, 1984 pp 449-456

TEXT OF ENGLISH ABSTRACT: In this article, the restraint of the spontaneous tearing modes caused by RHF is analyzed and calculated by solving the resistive MHD equations. We prove that the growth rate of the tearing modes of $m = 2$ can be reduced about two times by the helical fields. The restraint of the tearing modes by the boundary controlled field is also discussed and calculated numerically.

AUTHOR: QI Xiazhi [2058 7209 2655]
ZHENG Shaobai [6774 1421 4101]

ORG: Both of the Institute of Physics, Chinese Academy of Sciences

TITLE: "Soft X-Ray Emission and Its Fluctuation in CT-6B Tokamak"

SOURCE: Beijing WULI XUEBAO [ACTA PHYSICA SINICA] in Chinese No 4, 1984 pp 465-471

TEXT OF ENGLISH ABSTRACT: Soft X-ray diagnosis is an important method in the research of tokamak plasma instability. In this paper, we give the results of soft X-ray measurement in CT-6B tokamak by using Au(Si) surface barrier detector array, and present the spatial distributions of soft X-ray emission for various plasma instabilities in our device.

9717
CSO: 4009/100

END